Norwegian
Meteorological
Institute

METreport

No. 6/2026
ISSN 2387-4201
Open

Projected Mean Temperatures over India under RCP Scenarios

A Comparison of Statistical and Dynamical Downscaling

Abdelkader Mezghani, Øivind Hodneborg, Rasmus E. Benestad, Frode Stordal, Kajsa M. Parding, Janna Sillmann, and Sukumaran Sandeep

Title **Projected Mean Temperatures over India under RCP Scenarios: A Comparison of Statistical and Dynamical Downscaling**	**Date** 19.06.2026
Section Climate Department	**Report no.** No. 6/2026
Author(s) and Affiliation(s) Abdelkader Mezghani, Norwegian Meteorological Institute Øivind Hodneborg, CICERO Rasmus E. Benestad, Norwegian Meteorological Institute Frode Stordal, University of Oslo, Kajsa M. Parding, Norwegian Meteorological Institute Janna Sillmann, University of Hamburg, Sukumaran Sandeep, Indian Institute of Technology	**DOI** -
Classification ● Free ○ Restricted	**License** Open
Client(s) and/or project number Norwegian Research Council under the grant number 244551	**Client's reference** [Client's reference]

Abstract

We evaluate and compare two downscaling methods for reproducing observed temperature statistics across weather stations in India: (i) a dynamical downscaling approach using the Weather Research and Forecasting (WRF) model, and (ii) an Empirical–Statistical Downscaling (ESD) method. Both methods are driven by the same global climate model, CESM1-CAM4, allowing a consistent evaluation. Owing to its computational efficiency, the ESD method is also applied to the full CMIP5 multi-model ensemble to explore a broader range of climate futures.

Our analysis includes multi-scale evaluation at global, regional, and local levels, with a focus on seasonal and annual mean air temperature. Once validated, both methods are used to assess projected temperature changes at national and station scales. Despite a modest cold bias in WRF simulations (less than 0.5°C), both downscaling approaches project annual warming of approximately 1.5±0.5°C by 2041–2060 and 3.0±1.0°C by 2081–2100 under RCP8.5. Seasonal warming may reach up to 10°C in parts of India, indicating significant potential impacts on health, agriculture, and infrastructure.

Keywords

Climate, Future Temperature Projections, Empirical Statistical Downscaling, Weather Research and Forecasting Model, Multi-Scale Evaluation, Statistical Modeling, Indian Peninsula.

Disciplinary signature	Anita Verpe Dyrrdal Responsible signature

Abstract

We evaluate and compare two downscaling methods for reproducing observed temperature statistics across weather stations in India: (i) a dynamical downscaling approach using the Weather Research and Forecasting (WRF) model, and (ii) an Empirical–Statistical Downscaling (ESD) method. Both methods are driven by the same global climate model, CESM1-CAM4, allowing a consistent evaluation. Owing to its computational efficiency, the ESD method is also applied to the full CMIP5 multi-model ensemble to explore a broader range of climate futures.

Our analysis includes multi-scale evaluation at global, regional, and local levels, with a focus on seasonal and annual mean air temperature. Once validated, both methods are used to assess projected temperature changes at national and station scales. Despite a modest cold bias in WRF simulations (less than 0.5°C), both downscaling approaches project annual warming of approximately 1.5±0.5°C by 2041–2060 and 3.0±1.0°C by 2081–2100 under RCP8.5. Seasonal warming may reach up to 10°C in parts of India, indicating significant potential impacts on health, agriculture, and infrastructure.

Contents

1 Introduction

The exploitation of fossil energy sources, and the associated emission of CO_2 into the atmosphere, has over time resulted in global warming (Stocker et al., 2013). The way global warming affects society varies from place to place. In India, for instance, people have already experienced more frequent deadly heatwaves, such as one in 2015, which killed thousands of people across the country (Nageswararao et al., 2020).

Undoubtedly, India is under pressure to mitigate climate change, but it also needs to adapt to increased temperatures and associated consequences (Dileepkumar et al., 2018; Rohini et al., 2019; Kumar et al., 2023a). Even if greenhouse gas emissions were reduced, delayed effects of historic emissions due to the thermal inertia of the world oceans would continue to warm the planet for a long time (Kovats and Akhtar, 2008). One conclusion of a recent special report from the Intergovernmental Panel on Climate Change (IPCC) was that it may still be possible to avoid a future climate that is more than 1.5 °C warmer than pre-industrial times, although this seems increasingly unlikely (Allen et al., 2018). Nevertheless, countries such as India need to take immediate measures to adapt to a new climate (Dhara et al., 2020).

1.1 Historical Temperature Trends in India

There have been various studies published on historical trends in mean temperature over India (Ji et al., 2014; Gutiérrez et al., 2021). For example, Lal (2003) examined Indian meteorological data from more than 25 weather stations over the period 1881–2001 and found a significant annual mean warming rate of approximately 0.5–0.7 °C per century over the last hundred years. Another study by Arora et al. (2005), based on recorded temperatures at 125 stations distributed across India, also indicated that the annual mean temperature had increased by 0.42 °C during the last century with seasonal mean temperatures increasing by 0.94 °C for the post-monsoon season (October–November) and by 1.1 °C for the winter season (December–February). Their study also revealed stronger warming in southern and western India, by about 1.06 and 0.36 °C per century, respectively, and even negative temperature trends down to -0.38 °C per century in northern areas of the Indian plains. Later, Sanjay et al. (2020a) confirmed these findings based on a much denser meteorological network including more than 300 stations. They pointed out that, over the last century, temperatures increased by about 0.9 and 1.1 °C per century during winter and post-monsoon seasons, respectively, whereas during pre-monsoon (March–May) and monsoon (June–September) months, the warming was less pronounced—about 0.3 °C and 0.4 °C per century—with strong geographical variations. Kothawale et al. (2005) also revealed a substantial acceleration in historical trends over India, noting that during the more recent decades (1971–2003), the warming rate increased to approximately 2.2 °C per century, significantly higher than the trend over the past hundred years. A recent high-resolution assessment by Kumar et al. (2023a) further confirmed widespread warming over India, highlighting intensifying trends during the post-monsoon and winter seasons. A more recent work by Ravindra et al. (2024) shows that India has already experienced its hottest years on record (2016 and 2020) and projects a further rise in summer temperatures by 3–5 °C by 2100 under high-emission scenarios. The study emphasizes significant intensification of heatwaves, driven by both regional warming and large-scale atmospheric dynamics, with particularly severe impacts expected in northern and central India. Additionally, recent studies based on CMIP6 projections have provided updated insights into temperature changes over India. For instance, Shukla et al. (2024) found that under high-emission scenarios, extreme heat conditions in India are likely to intensify significantly by the end of the century, with critical implications for human health and agriculture. Similarly, Kumar et al. (2023b) highlighted a substantial increase in surface temperature variability over India, emphasizing the need for targeted adaptation measures. Patel et al. (2023) demonstrated that CMIP6 models capture the observed warming trends over India better than previous model generations, particularly for extreme temperature events. Moreover, Verma et al. (2023) found that regional temperature projections from CMIP6 scenarios show a stronger agreement with observed trends, suggesting higher confidence in future temperature projections under various emission scenarios. Increasing temperatures in India will likely have dire consequences for various sectors, such as health, agriculture, and transport (IPCC, 2012). Thus, reliable local estimates of future changes in temperature are needed for impact studies to facilitate adaptation and mitigation measures.

1.2 The Need for Downscaling in Climate Studies

Global climate models are our best means for providing an outlook of plausible future climate outcomes (IPCC, 2001), however, they are limited in terms of their ability to provide details about regional and local scales (Takayabu et al., 2015). Hence, downscaling continues to be used as a key approach to provide local climate information that better fits the requirements of impact studies (Benestad, 2016). The need for downscaling can be attributed to the coarse resolution of global climate models and simplifications of complex processes, which are necessary due to the high computational demand of global climate simulations. All climate models have a minimum skillful scale (Takayabu et al., 2015), and the main rationale for downscaling is to use the large-scale aspects that the global climate models are able to skillfully simulate and combine it with information on how the local-scale aspects depend on the large scales and the ambient geography.

There are two widely used techniques of scaling down large scale climatic features to regional or local scales: Empirical-Statistical downscaling (ESD) and Dynamical Downscaling (DD). On the one hand, ESD-based methods establish statistical connections between predicted local climate variables, such as recorded temperatures at weather stations, and atmospheric climate variables or indices derived from or modeled at the large scale (resolution of about a few hundreds of kilometers). On the other hand, Dynamical downscaling uses regional climate models (RCMs) based on thermodynamic principles and physical processes typically simulated on high spatial resolution ($\sim$ few tens of kilometers or less). Both methods include local geographical features such as topography, distance to the coast, etc.

Various ESD methods have been used to downscale and project the temperature for different catchments across India. For instance, Ghosh and Mujumdar (2008) applied statistical downscaling based on sparse Bayesian learning and Relevance Vector Machine to model stream flow at river basin scale for the monsoon period. Another study of Anandhi et al. (2009) applied a support vector machine to scale down surface temperature to the catchment of Malaprabha reservoir in the Karnataka state of India. Later, Goyal and Ojha (2012) developed statistical downscaling models using Linear Multiple Regression (LMR) and artificial neural networks to produce projections of mean monthly maximum and minimum temperatures for the Pichola lake catchment in Rajasthan State in India. Mahmood and Babel (2013) evaluated statistical models for downscaling temperature and precipitation in the upper Jhelum river basin underparts of Pakistan and India. Recently, Duhan and Pandey (2015) developed various statistical downscaling models to produce projections of monthly maximum and minimum air temperature for three stations in Tons River basin, a sub-basin of the Ganges River in Central India. All the above mentioned studies have applied statistical downscaling to isolated or small catchments in India and it is challenging to draw a general picture of future temperature trends in India due to the variety of data sets, time periods, methods, and case studies used. Parallel to the ESD applications, several model studies based on dynamical downscaling on a regional scale over India have been performed using different Regional Climate Models (RCMs).

Several multi-model RCM experiments covering the region of India have been performed, most of them in the framework of the Coordinated Regional climate Downscaling Experiment (CORDEX, Giorgi et al. (2009)). Such studies include several models, mostly run on 50 km resolution; RegCM4 (Giorgi et al., 2012), HadRM3 (Jones, 2004), COSMO-CLM (Steppeler et al., 2003; Velásquez et al., 2020), SMHI-RCA4 (Samuelsson et al., 2011), REMO (Jacob et al., 2012), LMDZ4 (Sabin et al., 2013), and CCAM (Evans et al., 2016). On the one hand, Mishra Vimal et al. (2014); Mishra et al. (2018) and Varikoden et al. (2018) focused on the past using re-analyses data as boundary conditions to validate their models and explore the added value of regional downscaling. For instance, Mishra et al. (2018) found that RCMs generally improve the spatial distribution of surface air temperature during JJAS season albeit negative biases in the magnitude after downscaling reaching down to 5 °C in some areas. They also found strong spatial variations of the projected temperatures with higher changes in the northernmost parts of Indian land, the Himalayan foothills, and northeastern parts of India. On the other hand, Kumar et al. (2013) in addition to simulations of the past, projected future climate in a 25 km resolution. Adopting the SRES A1B emission scenario they estimated warming over India to be about 1.5 °C and 3.9 °C at the end of 2050 and the end of the 21st century, respectively, with respect to the base period 1970-1999. The RCM studies of the future mentioned here have downscaled a variety of GCMs. Also, Coppola et al. (2014) and Giorgi et al. (2014) studied average and extreme climate from 1970 to 2100 with the RegCM4 model (Giorgi et al., 2012) with a resolution of 50 km using the Representative Concentration Pathways RCP4.5 and RCP8.5 (van Vuuren et al., 2011) . Using the same model and time period, Dash et al. (2015) estimated that towards the end of this century the Indian subcontinent will warm up by 4 to 5 °C compared to 1975-2004, relatively more on the western side. Bal et al. (2016) assessed projected minimum and maximum temperature changes over India using the PRECIS regional climate model in a resolution of 25 km and assuming emission rates provided within the special report on emission scenarios (SRES) A1B. They projected an overall increase in maximum temperature within the range 2.5 °C to 4.4 °C, also by the end of this century, with respect to the baseline period 1975-2005. More recently, Sanjay et al. (2020b) has confirmed those changes based on a larger downscaled ensemble of global (CMIP5) and regional (CORDEX–South Asia) climate models using both physic and statistic based approaches. They found that, relative to the period 1976–2005, the mean surface air temperature over India is projected to be in the range of 1.4–4.4°C by 2070–2099, regardless of the radiative concentration pathway. Furthermore, the Weather Research and Forecasting (WRF) model has been widely applied for long-term climate simulations over India. For example, Sharma et al. (2021) analyzed the model's performance in simulating extreme heat events, while Choudhury et al. (2021) highlighted its utility in capturing regional monsoon variations. Additionally, Rao et al. (2018) and Kumar et al. (2012b) utilized the WRF model for high-resolution projections over different Indian subregions, demonstrating its reliability in assessing future climate conditions.

In this study, we performed and evaluated a set of experiments based on two downscaling methods, each employing a variety of data sets, applied to the entire Indian peninsula. Firstly, the Weather Research and Forecasting (WRF) model (Skamarock and Klemp, 2008) was used to downscale historical and future climate over India. The WRF model in climate mode has previously been used in historical studies over India of a few selected years, such as Kumar et al. (2012a) studying climate and chemistry in 2008, and Devanand et al. (2018) investigating the conditions during the three contrasting monsoon rainfall years 1994 (excess rainfall), 2002 (deficit), and 2010 (normal). Secondly, the ESD method proposed by Benestad et al. (2016) was used, which also has demonstrated skillful predictions across various European regions and elsewhere both in terms of spatial and temporal distributions of temperatures at the local scale (Benestad, 2011). The strength of this method is that it builds on common ground between GCMs and reanalyses data sets both in space and time via establishment of common Empirical Orthogonal Functions (common-EOFs) that are further used along with appropriate regression models to downscale future global climate scenarios at individual sites. Benestad et al. (2015) showed that the method is improved by application to an entire set of weather stations across a region. Finally, to evaluate the robustness of the temperature change signal over India, the ESD projections of temperature were compared with the results of dynamical downscaling of the same GCM simulations using the WRF-CAM4 model with a horizontal grid resolution of 45 km and 15 km, respectively, and interpolated to meteorological weather stations across India.

1.3 Research Framework

To address the challenges of projecting regional temperature changes and their implications for the Indian peninsula, this study employs a comprehensive research framework involving multiple datasets, three levels of evaluation (global, regional, and local), and two distinct downscaling methods.

The foundation of this study is the integration of multiple datasets, including observational meteorological data, reanalysis datasets, and outputs from global climate models (GCMs). These datasets provide a robust basis for analyzing historical and future climate conditions across the Indian peninsula and are essential for validating and comparing the downscaling methods. The study incorporates three levels of evaluation: global, regional, and local. At each level, the datasets and downscaled results are adapted accordingly to ensure specificity in the analysis.

Two complementary downscaling methods are employed in this study. The first is the Weather Research and Forecasting (WRF) model (Skamarock and Klemp, 2008), a dynamical downscaling approach used to simulate historical and future climate conditions. WRF simulations are conducted at horizontal resolutions of 45 km and 15 km and are interpolated to meteorological weather stations to enable evaluation at the local scale. The second method is Empirical-Statistical Downscaling (ESD) as proposed by Benestad et al. (2016), which leverages statistical connections between GCM outputs and local meteorological data. ESD projections are gridded to the same spatial resolution as WRF to allow for consistent comparison across regional and local scales. This ensures that each level of evaluation—global, regional, and local—is conducted with tailored datasets and downscaled results.

The downscaled temperature projections are evaluated across the Indian peninsula, spanning both historical and future climate scenarios. These evaluations enable an assessment of the robustness of temperature change signals at local and regional scales, highlighting the ability of each method to reproduce observed trends and project future changes.

Finally, the results from the two downscaling methods are compared to assess their reliability and robustness in producing actionable temperature projections. This research framework provides a systematic approach to evaluating downscaling methods and their applicability in climate impact studies, with implications for adaptation strategies in key sectors such as agriculture, health, and water resources.

1.4 Organization of the MET Report

This MET report is organised as follows. Section 2 presents the various types of climate data sets used in the study. The downscaling methods and experiments used to produce projected temperature are described in Section 3. Results of our study are described in Section 4 followed by a discussion and some conclusions presented in sections 5 and 6, respectively.

2 Data sets and climate simulations

2.1 Meteorological Weather Stations in India

The analysis of historical temperature trends in this study was based on the daily mean temperature derived from recorded daily minimum and maximum temperatures at a selection of weather stations across India. The selection was based on the criteria that the data (i) were open access, (ii) 30-years minimum length, and (iii) covering the recent period 1986–2005. The mean temperature values were calculated as the average between daily minimum and maximum values at each individual weather station. The 31 weather stations that were selected are listed and described in Table 1 and displayed on the map in Figure 2.

We used the 'esd' R-package developed at the Norwegian Meteorological Institute (Benestad et al., 2014) to, first, retrieve the time series from the Global Historical Climate Network - Daily (GHCND) database (Menne et al., 2012) and, second, process and visualise the content of the data. A PCA-based approach following Benestad et al. (2016) was used to fill in the gaps found in the retrieved data sets (last column in Table 1) prior to downscaling.

2.2 IMD Gridded Dataset

The India Meteorological Department (IMD) provides station-based gridded temperature products that are widely used for climate studies and model evaluation over India. For this study, we used the IMD gridded daily maximum and minimum temperature dataset developed by Srivastava et al. (2009), which is a station-interpolated product at 1° × 1° resolution covering the Indian landmass for the period 1969–2005. The dataset was created from 395 quality-controlled IMD meteorological stations using a modified Shepard's angular distance weighting algorithm (a variant of inverse-distance weighting). Cross-validation errors were reported to be less than 0.5 °C.

The IMD gridded temperature dataset is particularly advantageous for regional climate studies because it provides spatially complete, continuous fields derived from station observations, even in regions with relatively sparse station coverage. Although different IMD products span different periods (e.g., the Srivastava et al. (2009) product covers 1969–2005), IMD also maintains longer station records for certain variables and periods. The gridding procedures and quality control applied to these products are well-documented in IMD/MAUSAM materials and Srivastava et al. (2009).

For this study, daily mean temperature was derived as the arithmetic average of daily maximum and minimum temperatures at each grid cell. The gridded data were used to validate downscaled temperature projections and to assess the models' ability to reproduce spatial patterns and temporal trends of historical variability. Widely used and evaluated in India-focused studies of temperature trends, heatwaves, and regional variability (e.g., Pai et al., 2013; Kothawale et al., 2005), the IMD gridded dataset's station-based nature makes it suitable for comparisons with reanalyses and station observations. This enables a comprehensive assessment of the performance of dynamical and statistical downscaling methods over India.

2.3 Reanalyses data sets

Four reanalyses were used in the empirical-statistical and dynamical model calibration. We extracted values of seasonal 2m air temperature (T_{2m}) from the ERA-interim (Hersbach et al., 2020) and ERA5 (Hersbach and Dee, 2016) reanalyses from the European Centre for Medium-range Forecasts (ECMWF) and the Modern-Era Retrospective analysis for Research and Applications (MERRA) produced by NASA's Global Modeling and Assimilation Office (Rienecker et al., 2011). The seasonal mean T_{2m} for the period 1979–2018 and the domain 55–100°E/5–35°N were used to extract predictors for ESD model calibration and validation. The spatial resolution of ERA5 is ∼32 km, substantially higher than for the ERA-interim reanalysis at 0.75° (∼78 km) and MERRA (∼50 km). The oceanic region is included to provide boundary conditions for both downscaling methods, as these rely on large-scale atmospheric variables as input/initial conditions. However, for local-scale assessments, the oceanic region is excluded, as the evaluation is based on station data over the landmass.

Reanalyses from the NCEP/NCAR Reanalysis Project (NNRP), developed by the National Centers for Environmental Prediction (NCEP) with a horizontal resolution of approximately ∼250 km (Kalnay et al., 1996), were included primarily to set the boundary conditions for the WRF simulations (see Section 3.1) and for evaluation purposes.

2.4 The CMIP5 global climate model ensemble

Global climate model (GCM) simulations of temperature from the Coupled Model Intercomparison Project phase 5 (CMIP5; Meehl et al. (2007)) were used to represent both historical and future climate conditions, forming the basis for downscaling temperature over India. Historical simulations represent past climate conditions up to the year 2005, while future simulations are driven by Representative Concentration Pathways (RCPs)–emission scenarios that outline possible trajectories of greenhouse gas concentrations to the year 2100.

The high-emission scenario (RCP8.5) was assumed in order to drive the regional and local dynamical and empirical-statistical downscaling models (IPCC, 2013). In addition to the CMIP5 GCM ensemble, we performed a more detailed analysis of a single simulation of the Community Earth System Model (CESM), which includes both historical and RCP8.5 future simulations.

2.5 The Community Earth System Model – Community Atmosphere Model version 4

Meteorological initial and boundary conditions to WRF come from simulations with the National Center for Atmospheric Research (NCAR) Community Earth System Model (CESM) version 1.0.4 (Gent et al., 2011). The CESM was set up with the CAM version 4 (Neale et al., 2013b). Additional details on these simulations can be found in Hodnebrog et al. (2019). It should be noted that the CAM4 module is an earlier version of CAM5 on which the CMIP5 ensemble is based (see Section 4). One difference between CAM4 and the following generation CAM5 is that CAM4 does not include indirect aerosol effects.

The horizontal resolution of the CESM1-CAM4 is 1.9 ° by 2.5 °($\sim$200 km) and the number of vertical levels is 26. These simulations cover the period 1850–2100, with historical simulations to the year 2005 and future projection driven by the high RCP8.5 emission scenario from the year 2006 and onward.

The CESM1-CAM4 results were used in both downscaling approaches as follows. In the DD, they were used to set the lateral boundary conditions for the WRF model (Section 3.1), while in the ESD, they were used to represent the predictors in the simulation framework (Section 3.2).

3 Downscaling Methods and Experiments

3.1 Dynamical Downscaling

The CESM1-CAM4 model outputs and NNRP data (as described in Section 2) were used as inputs for dynamical downscaling of daily temperature over India using the WRF model (version 3.7.1) (Skamarock and Klemp, 2008). The WRF setup consisted of two nested domains with 35 vertical levels. The outer domain, with a resolution of 45 km × 45 km, encompassed much of South Asia and incorporated spectral nudging for temperature, horizontal winds, and geopotential height above the planetary boundary layer. Spectral nudging was applied to wavenumbers ≤ 6, corresponding to wavelengths greater than 1,000 km, with a relaxation coefficient of 0.0003. The inner domain, with a resolution of 15 km × 15 km, covered the Indian subcontinent and the Tibetan Plateau, without spectral nudging.

The initial conditions (IC) and boundary conditions (BC) for the dynamical downscaling were specified at a 6-hour interval. This time interval ensures that the WRF model receives sufficient information from the driving data (e.g., CESM1-CAM4 outputs or NNRP reanalysis) to maintain consistency with the large-scale atmospheric state while allowing the model to dynamically simulate smaller-scale features. Lateral boundary conditions were updated every 6 hours in all simulations. Sea surface temperatures (SSTs) were also prescribed and updated daily using data from CESM1-CAM4.

The model configuration employed the CAM radiation scheme (Collins et al., 2004), the WSM 6-class graupel microphysics scheme (Hong and Lim, 2006), the Kain–Fritsch cumulus parameterization scheme (Kain and Fritsch, 1993), the YSU planetary boundary layer (PBL) scheme (Hong et al., 2006), the revised MM5 Monin–Obukhov surface layer scheme (Jiménez et al., 2011), and the unified Noah land surface model (LSM) (Tewari et al., 2004). Horizontal diffusion was applied with `diff_opt = 1` and `km_opt = 4`, and turbulence mixing was configured for first-order closure.

WRF was run for two 20-year periods: 1986–2005 (historical) and 2041–2060 (near-future) under the high-emission RCP8.5 scenario. Each year was simulated individually, with initialization in December of the preceding year and a one-month spin-up. For historical simulations, additional experiments were conducted using initial and boundary conditions from the NNRP dataset. Lateral boundary conditions were handled using a relaxation zone of 5 grid points.

3.2 Empirical-Statistical Downscaling

The empirical-statistical downscaling involved a stepwise multiple linear regression,

$$y_j = \beta_0 + \sum_{i=1}^{m} \beta_i x_i,$$

where the predictands y_j are the principal components (PCs) obtained from a Principal Component Analysis (PCA) applied to weather station datasets of seasonal mean temperature (Benestad et al., 2015), and the predictors x_i are common Empirical Orthogonal Functions (common EOFs; Suarez-Gutierrez et al. (2021)) derived from a combined data matrix of seasonal temperature anomalies from both reanalysis and global climate model outputs. Here, the regression was performed on $j \in [1, n]$ PCA modes and $i \in [1, m]$ common EOFs, with $n = 5$ and $m = 20$, accounting for more than 70% of the variance in the data. A stepwise selection process using the Akaike Information Criterion (AIC; Akaike (1974)) was applied to retain only statistically significant predictors in the regression models. It is worth noting that while the EOF analysis identifies dominant large-scale climate patterns over the region of interest, the PCA captures local climatic variability specific to the weather stations.

The ESD framework was initially applied to downscale large-scale temperature fields simulated by the CESM1-CAM4 model combined with ERA-Interim reanalysis onto Indian weather stations. Due to their computational efficiency, the ESD experiments were further extended to include the full set of reanalyses and CMIP5 global climate models, as described in Section 2. Calibration periods for the various ESD experiments differed according to the availability of weather station and reanalysis data.

3.3 Summary of the downscaling experiments

Figure 3 describes the various downscaling experiments that were used to simulate historical and future mean temperature at selected weather stations and consist of:

- WRF model forced by NNRP on a 45 km horizontal grid resolution.
- WRF model forced by NNRP on a 15 km horizontal grid resolution.
- WRF model forced by the CESM1-CAM4 on a 45 km horizontal grid resolution.
- WRF model forced by the CESM1-CAM4 on a 15 km horizontal grid resolution.
- ESD forced by the CESM1-CAM4 at selected stations.
- ESD forced by the CMIP5 multi-model ensemble, including the CESM1-CAM5.

4 Results

The results presented in this section are structured to provide a comprehensive evaluation of temperature data and downscaling methods across multiple scales and approaches. We begin by analyzing thermometer measurements from selected weather stations across India, focusing on spatial coverage, data completeness, and climatological gradients over the 1986–2005 reference period (Table 1, Figure 2). Subsequently, we assess large-scale temperature anomalies from CMIP5 global climate models for the broader domain (55–100°E, 5–35°N), comparing outcomes from three emission scenarios (RCP2.6, RCP4.5, RCP8.5) after applying a Gaussian temporal smoothing (Figure 4). We further evaluate the regional performance of the CESM1-CAM4 model over India by comparing simulated seasonal and annual temperatures to multiple reanalysis datasets (ERA-Interim, ERA5, MERRA, and NNRP) and quantifying biases relative to the multi-reanalysis ensemble mean (Table 3). Finally, we evaluate the performance of two downscaling methods—dynamic downscaling using the WRF model at two spatial resolutions (45 km and 15 km) and empirical–statistical downscaling (ESD)—by assessing biases at both regional and station scales in comparison to reference datasets (e.g., NNRP, IMD gridded data, and station observations). This multi-scalar approach provides a detailed evaluation of the strengths and limitations of each method, highlighting their suitability for resolving fine-scale temperature variability and long-term climate trends over India.

4.1 Evaluation of the various data sets

4.1.1 Thermometer measurements over India

Table 1 presents the general characteristics of selected weather stations in India and Figure 2 shows their spatial distribution across the country. Table 1 also indicates the gaps in the data sets in terms of percentage of missing values which can be, in some locations, more than 50 % (e.g. 'Jaipur/SA').

Table 1 also provides the annual mean daily temperature averaged over the period 1986–2005 at the different sites, which ranges from 24.4 °C recorded at Gauhati located in the north-eastern side of the country to 29.5 °C recorded at 'Nellore' near the southeastern coast of India (Table 1). It also depicts the various spatial characteristics influencing the temperature variability in the region such as the south-north and east-west gradients, the influence of the Arabian Sea, the Indian Ocean, and the Bay of Bengal distinguishing coastal sites and the inland sites from the mountains (Figure 2).

4.1.2 CMIP5 global temperature anomalies over India

Figure 4 presents the annual mean temperature anomalies relative to the baseline period 1986–2005 for the domain 55–100°E/5–35°N, which includes India. These anomalies are shown for three emission scenarios—RCP2.6, RCP4.5, and RCP8.5—using the NNRP global temperature dataset as a reference. Both modeled and reference data were interpolated onto the common NNRP grid (2.5 °× 2.5 °) before averaging over the large-scale spatial domain covering India (Figure 2).

To reduce noise in the annual mean climate signal, a Gaussian filter with a 20-year temporal window ($w = 20$ years) was applied. The multi-model ensemble spread around the mean was represented using a standard error of $0.7 \times \sigma_{ens}$, where σ_{ens} is the standard deviation of the full ensemble mean. This approach reduced the weight of extreme values or outliers, focusing instead on the core variability of the data.

The comparison illustrates the range of potential future warming across different emission scenarios, with RCP8.5 exhibiting the largest anomalies due to its assumption of sustained high greenhouse gas emissions. Projections show a gradual warming of approximately 1 °C under the low-emission scenario RCP2.6, intensifying to around 2 °C and 5 °C by the end of the 21st century under the intermediate (RCP4.5) and high-emission (RCP8.5) scenarios, respectively.

In the following analysis, we focus on the high-emission RCP8.5 scenario as a worst-case pathway to assess the impacts of global temperature changes on local climates at the selected stations listed in Table 1. Further evaluation of CESM1-CAM4 outputs, which serve as lateral boundary conditions for the WRF simulations, is provided in the next section.

4.1.3 CESM1-CAM4 regional performance over India

To evaluate the performance of the CESM1-CAM4 model over India, we first estimated seasonal and annual regional mean temperatures averaged over the domain encompassing India using various reanalysis data sources, including ERAINT, ERA5, MERRA, and NNRP. The model results demonstrated good agreement with all reanalysis data sets in reproducing the regional mean seasonal cycle of surface air temperature over the selected spatial domain, with a relatively small multi-reanalysis ensemble spread of approximately +0.4 to +0.5 °C on both seasonal and annual scales.

Next, we computed the bias between the regional temperatures simulated by the CESM1-CAM4 model and the multi-reanalysis ensemble mean, which was taken as the reference. The results, summarized in Table 3, indicate good agreement between the modeled and reference data sets at both seasonal and annual scales. Specifically, small cold biases were observed in DJF and MAM seasons, reaching down to −0.6 °C and −0.1 °C, respectively. Conversely, in JJA and SON, the CESM1-CAM4 model exhibited a modest positive bias of approximately +0.7 °C and +0.6 °C, respectively. Importantly, these biases are of similar magnitude to the multi-reanalysis ensemble spread (±0.5 °C), suggesting that the signal-to-noise ratio is close to unity.

When compared to its successor, CESM1-CAM5, the CESM1-CAM4 model exhibits slightly cooler temperatures under the high-emission RCP8.5 scenario. CESM1-CAM5 simulations closely align with the CMIP5 multi-model ensemble mean, while CESM1-CAM4 projects a slightly cooler climate, consistent with the findings of Meehl et al. (2013). This difference can likely be attributed to advancements in physical parameterizations and cloud-aerosol interactions implemented in CESM1-CAM5, which contribute to its improved performance compared to CESM1-CAM4. Nonetheless, CESM1-CAM4 demonstrates sufficient accuracy in representing regional mean temperatures over India, making it a reliable choice for providing boundary conditions for the WRF simulations.

4.2 Evaluation of Downscaling Methods

To evaluate the performance of the downscaling methods, temperature biases were assessed at regional and local scales across both annual and seasonal levels for the reference period 1986–2005. Regional biases reflect the difference between simulated and reference data (NNRP and IMD gridded datasets), spatially averaged over the domain (55–100°E, 5–35°N). Local-level evaluation was conducted by comparing station observations with simulated values (Table 1); for WRF simulations, this required bilinear interpolation to specific station coordinates, whereas for ESD, a rigorous five-fold cross-validation procedure was performed to ensure model reliability across the entire calibration period.

4.2.1 WRF Model Evaluation

Annual Biases

Regional analysis (Figure 5) indicates that WRF effectively captures large-scale thermal patterns, though significant deviations ($\pm\ 10$°C) are observed in the Himalayas. These biases are primarily attributed to the coarse resolution of the NNRP reference data (2.5° × 2.5° ≈ 250 km), which inadequately resolves the region's complex topography. When evaluated against the IMD gridded dataset (Figure 6, 1° × 1° ≈ 100 km), WRF simulations exhibit lower cold biases in the Himalayan region, exceeding ± 5°C, even in the finer domain (D02: 15 km). In flatter regions such as central and coastal India, the biases are smaller. For the coarser domain (D01: 45 km), biases typically range between -3°C and $+3$°C, while the finer domain (D02) reduces these biases to within -2°C to $+2$°C.

At the station level (Table 5), WRF/NNRP simulations at 15 km resolution show an average annual bias of -0.4°C, an improvement over the 45 km resolution (-1.2°C). Similarly, WRF/CAM4 simulations exhibit an average bias of -0.6°C at 15 km, compared to -0.9°C at 45 km. However, WRF simulations exhibit higher variability in biases (standard deviation of 1.3°C) compared to ESD simulations, which show much smaller biases (-0.3°C for CAM4 and 0.0°C for CAM5) and minimal variability (standard deviation of 0.1°C).

Seasonal Biases

Seasonal biases reveal significant variability in WRF performance across both regions and seasons (Tables 6a–6b). Systematic cold biases dominate the DJF season (average bias -1.5°C), while MAM exhibits the largest variability, with seasonal standard deviations reaching up to 2.0°C. Coastal stations in southern India (e.g., Nellore, Tiruchchirapalli) show pronounced cold biases during MAM, while localized warm biases are evident in the Indo-Gangetic Plain during JJA, particularly at stations such as New Delhi/S (up to $+4.3$°C).

The IMD dataset comparison reveals that WRF/NNRP simulations tend to exhibit larger cold biases in regions with sparse observational coverage, such as northeastern India and the Himalayas, while WRF/CAM4 simulations show smaller cold biases in these regions but higher warm biases in the Indo-Gangetic Plain. Both WRF/NNRP and WRF/CAM4 simulations struggle to resolve biases in coastal zones, though the finer resolution (15 km) consistently reduces errors compared to the coarser resolution (45 km).

Despite these challenges, WRF simulations offer valuable insights into fine-scale temperature patterns, complementing the more consistent but coarser ESD simulations.

4.2.2 ESD Model Evaluation

Annual Biases

The ESD simulations, driven by CESM1-CAM4 and CESM1-CAM5, exhibit smaller annual biases compared to WRF simulations (Table 5). On average, ESD simulations driven by CAM4 have an annual bias of -0.3°C, while those driven by CAM5 show negligible biases (0.0°C). Furthermore, ESD simulations show minimal variability across stations, with a standard deviation of just 0.1°C for both CAM4 and CAM5. This highlights the strength of statistical downscaling in reducing systematic biases.

At the station level, ESD biases remain consistently small across most locations. For example, coastal stations such as Nellore and Tiruchchirapalli exhibit biases close to 0.0°C, while inland stations such as New Delhi/S show slightly positive biases (up to $+0.1$°C). These results indicate that ESD performs well across both coastal and inland regions, with smaller biases and less variability than WRF.

Seasonal Biases

Seasonal biases in ESD simulations (Tables 6a and 6b) are also smaller and less variable compared to WRF. For example, in DJF, ESD simulations driven by CAM5 show an average bias of -0.1°C, compared to -1.5°C in WRF simulations. Similarly, in MAM, ESD simulations exhibit much smaller standard deviations (0.1°C) compared to WRF (up to 2.0°C). These results highlight the ability of ESD to consistently reproduce seasonal temperature patterns with minimal errors.

4.2.3 Model Comparisons

WRF simulations at 15 km resolution (both NNRP and CAM4-driven) consistently improve over 45 km simulations, with average annual biases reducing from -1.2°C to -0.4°C for WRF/NNRP and from -0.9°C to -0.6°C for WRF/CAM4. However, ESD simulations demonstrate even smaller biases (-0.3°C for CAM4 and 0.0°C for CAM5) and minimal variability, highlighting the robustness of statistical downscaling in reducing systematic errors.

WRF exhibits significant variability in seasonal biases, with cold biases dominating DJF (-1.5°C on average) and warm biases dominating JJA (e.g., $+4.3$°C at New Delhi/S). In contrast, ESD remains consistent across all seasons, with biases generally within ±0.3°C.

The comparison between WRF and ESD reveals distinct strengths and weaknesses for each approach. WRF offers superior spatial resolution, enabling it to capture fine-scale temperature patterns, particularly in flatter regions. However, it struggles in regions with complex terrain or strong land-sea contrasts, leading to larger biases and higher variability, especially during certain seasons (e.g., MAM and JJA). In contrast, ESD produces smaller biases and less variability across both annual and seasonal scales, making it more consistent but less detailed spatially.

4.3 Projected Temperature Changes over Selected Stations in India

This section presents future projections of temperature changes at selected meteorological stations across India, derived from both dynamical (WRF) and empirical–statistical downscaling (ESD) methods under the high-emission RCP8.5 scenario. The analysis focuses on seasonal and annual mean temperature changes relative to the historical baseline period (1986–2005) for near-future (2041–2060) and, where available, far-future (2081–2100) time horizons. WRF simulations were conducted at two spatial resolutions (45 km and 15 km) using CESM1-CAM4 as the driving global climate model, while ESD projections were developed using statistically calibrated relationships between observed and modeled data. The results, summarized in Tables 7 and 8, provide insights into the spatial and temporal variability of projected warming across India, evaluating differences in regional sensitivity as well as the influence of model resolution and methodological approaches. This comparative assessment highlights both consistencies and discrepancies in the downscaled projections, providing a robust foundation for subsequent impact analyses.

4.3.1 WRF-CAM4 Projected Changes

Table 7 presents absolute temperature changes for 2041–2060 relative to the baseline period 1986–2005, as simulated by the WRF model driven by the global climate model CESM1-CAM4 at two resolutions (45 km and 15 km). Averaged across all sites, the WRF-driven simulations project an increase in annual mean temperature of approximately 1.4±0.1 °C and 1.3±0.1 °C for the 45 km and 15 km resolutions, respectively. Seasonal temperature increases vary between 1.1±0.2 and 1.6±0.4 °C, largely independent of resolution.

Spatial variability in projected warming is small, with a standard deviation below 0.4 °C. The strongest warming occurs in northern India, while southern regions exhibit comparatively lower temperature increases. For the 45 km runs, projected seasonal increases range from 1.1 °C (e.g., 'Nellore' station) to 2.3 °C (e.g., 'Ahmadabad' station) in DJF; 1.1 °C (e.g., 'Bombay/Santacruz') to 1.7 °C ('Jabalpur') in MAM; 0.7 °C ('Indore') to 1.4 °C ('Patna') in JJA; and 1.1 °C to 1.6 °C in SON.

Temperature changes from the 15 km simulations closely match those from the 45 km runs (differences less than 0.1 °C), suggesting that increased horizontal resolution—and the corresponding computational cost—does not significantly affect projected warming across Indian meteorological sites.

4.3.2 ESD Projected Changes

Like the WRF-driven projections, ESD-based future temperature changes were calculated as deviations from the historical period 1986–2005 on seasonal and annual scales (Table 8). The ESD projections extend to the end of the 21st century, providing longer-term outlooks.

Averaged over all sites, the ESD results indicate a warming of 1.5±0.5 °C by the near future (2041–2060) under the high-emission RCP8.5 scenario. This warming is projected to approximately double by 2081–2100, reaching 3±1.1 °C. Compared to the WRF-CAM4 projections, ESD simulations exhibit greater spatial variability, with site-to-site differences up to 2.3 °C in SON by the far future.

At individual stations, the highest warming occurs during SON, with temperature increases of 4.9 °C and 9.8 °C projected for the near and far future, respectively, at 'Gwalior' in northern India. Unexpectedly, slight temperature decreases (less than 0.3 °C) in JJA are projected at two high-elevation stations—Bhopal (523 m a.s.l.) and Indore (567 m a.s.l.)—both located in the desert region.

5 Discussion

5.1 Key Findings and Insights

This study highlights the complementary nature of Dynamical Downscaling (DD) and Empirical-Statistical Downscaling (ESD) approaches in capturing climate variability across spatial and temporal scales. At the global scale, CESM-CAM4 and CESM-CAM5 global climate model outputs demonstrated robust performance in reproducing temperature features over the Indian region, with seasonal and annual deviations within ±0.8 °C relative to the multi-reanalysis ensemble mean. These findings align with earlier studies (e.g., Gent et al., 2011; Neale et al., 2013a), which showed reliable performance of CESM for capturing large-scale climate features.

At the regional scale, WRF simulations revealed systematic cold biases of −1.6 to −0.5 °C, consistent with previous findings by Kumar et al. (2012a) and Thomas et al. (2016). However, substantial spatial variability in biases was observed, particularly in regions with complex topography such as the Himalayan foothills, where biases exceeded ±5 °C. This result is consistent with studies suggesting that coarse-resolution reanalysis datasets (e.g., NNRP) struggle to resolve fine-scale topographic effects (Majumdar et al., 2021; Laprise, 2008). These biases underscore the limitations of dynamical models in regions where topography and land-surface interactions play a critical role.

At the local scale, both DD and ESD approaches yielded broadly consistent warming trends, with mean annual temperature increases of approximately +1.3 °C (WRF-15 km) and +1.5 °C (ESD) projected for 2041–2060. Similar warming trends have been reported in other downscaling studies over South Asia (Dash et al., 2013; Krishnan et al., 2020). However, spatial variability was notably higher in ESD simulations (0.5–1.2 °C) compared to WRF-15 km (0.1–0.3 °C), suggesting that ESD may better preserve local-scale heterogeneities. This finding aligns with Tebaldi et al. (2009), who emphasized the ability of ESD methods to capture sub-grid variability.

5.2 Comparative Performance of DD and ESD

The study demonstrates the strengths and weaknesses of both approaches. DD, through the WRF model, provides superior spatial resolution and captures mesoscale processes more effectively, particularly in flatter regions, as shown in Mezghani et al. (2016) and Goyal et al. (2022). However, WRF struggles in areas with complex topography and exhibits systematic biases, likely propagated from boundary conditions or due to model physics, as noted in Laprise (2008) and Gao et al. (2017).

In contrast, ESD relies on long-term statistical relationships and consistently exhibits smaller biases across scales. Its ability to directly leverage station-level observations makes it particularly suited for evaluating localized climate variability. However, ESD's reliance on historical data for calibration may limit its applicability in regions where observational records are sparse or of poor quality, as highlighted in Wilby et al. (2004) and Hessami et al. (2008). Nonetheless, ESD has been shown to perform well across diverse climates and regions, including India (Mujumdar et al., 2012).

5.3 Implications for Downscaling Studies in India

The findings have significant implications for climate impact assessments in India. The systematic cold biases observed in WRF simulations over the Arabian Sea and the Himalayan region may affect projections of Indian monsoon dynamics, as previously noted by Sandeep et al. (2014) and Krishnan et al. (2016). Addressing these biases is critical, as they could influence hydrological and agricultural impact assessments, which depend on accurate monsoon projections. Improved parameterizations of surface fluxes and regional atmospheric dynamics in WRF are needed to address this issue (Gill et al., 2020).

Furthermore, the higher spatial variability in ESD simulations suggests that applying ESD methods to high-resolution gridded datasets, such as those developed by Srivastava et al. (2009), could enhance the representation of localized extremes, particularly in urban areas. Incorporating urban canopy and albedo effects in WRF (e.g., Bhati and Mohan, 2018; Chen et al., 2011) could further improve urban climate simulations, reducing warm biases in cities like Delhi, Lucknow, and Patna. This is particularly relevant given the rapid urbanization in India and the associated impacts on local and regional climates (Seto and Dhakal, 2012).

5.4 Limitations and Future Directions

Despite its contributions, this study has several limitations. The use of coarse-resolution reanalysis datasets (e.g., NNRP) as boundary conditions for WRF simulations likely contributed to the observed biases in regions with complex topography, as noted by Laprise (2008). Additionally, the limited availability and variable quality of Indian observational data pose significant challenges for both DD and ESD evaluations. Although high-resolution gridded datasets (Srivastava et al., 2009) are now accessible, direct station-level observations remain critical for rigorous model evaluation and validation. As Maraun (2016) noted, reliance on gridded datasets alone introduces uncertainties due to interpolation artifacts, which can propagate into downscaling evaluations.

Future research should prioritize integrating gridded products with station-level observations to enhance the robustness of downscaling evaluations (Mujumdar et al., 2012; Mezghani et al., 2019). Expanding ESD analyses to incorporate multiple GCMs from the CMIP5 or CMIP6 ensemble (Tebaldi et al., 2009; Krishnan et al., 2020) could provide more comprehensive uncertainty estimates. Additionally, exploring advanced bias correction methods (e.g., Cannon et al., 2015) and incorporating urban-specific processes in WRF could further improve the accuracy of regional and local climate simulations.

This study underscores the strengths of combining DD and ESD methods for climate downscaling in India. While DD offers high-resolution spatial detail, ESD provides consistent performance with minimal biases. Together, these approaches can provide a more holistic understanding of climate variability and trends, enabling more effective climate adaptation and mitigation planning for the region. Future efforts should focus on addressing systematic model biases, improving observational datasets, and refining methodologies to enhance the reliability of downscaling projections.

6 Conclusions

We evaluated temperature projections over India using two downscaling approaches: empirical-statistical downscaling (ESD) and dynamical downscaling. Both methods utilized outputs from the CESM-CAM4 global climate model (GCM), differing in training data and methodology. The ESD approach was trained on ERA-Interim reanalysis data to produce station-level projections, while dynamical downscaling employed the Weather Research and Forecasting (WRF) model driven by both NNRP and CESM1-CAM4 outputs at 45 km and 15 km horizontal resolutions (Table 9).

An initial global-scale evaluation over 55°–100°E and 5°–35°N—including the Indian subcontinent and surrounding seas—confirmed that the CMIP5 multi-model ensemble under RCP2.6, RCP4.5, and RCP8.5 scenarios realistically reproduced historical temperature anomalies. The RCP8.5 scenario projected the highest warming, with global temperature increases of approximately 5 ± 2 °C by 2081–2100, motivating our focus on this scenario as a worst-case pathway.

At the regional scale, CESM1-CAM4 demonstrated satisfactory skill in simulating historical absolute surface temperatures, with annual and seasonal biases of +0.2 °C and ± 0.8 °C relative to multi-reanalysis means (Table 3), supporting its use for downscaling.

Local-scale assessments revealed widespread increases in mean temperature across India on both annual and seasonal scales. Minor cooling (< 0.3 °C) during the monsoon season was projected at select stations (e.g., Indore and Bhopal). Spatial and seasonal variability was evident, with the largest warming at Gwalior (SON, 9.8 °C), Ahmedabad (SON, 8.1 °C), and Nagpur Sonega (DJF, 7.6 °C), as projected by ESD under RCP8.5 by late century. Generally, ESD projected larger temperature increases than WRF, while WRF simulations showed that increasing horizontal resolution from 45 km to 15 km had negligible impact on warming projections (< 0.1 °C difference).

Despite some historical biases in WRF-CAM4 at local sites, both downscaling methods consistently projected warming of about 1.5 °C by mid-century. Projections suggest warming may roughly double by 2100, with localized increases reaching up to 10 °C, posing potential risks to sensitive sectors such as agriculture. The CMIP5 multi-model ensemble further indicated that New Delhi could experience warming up to 7 °C by century's end under the worst-case scenario.

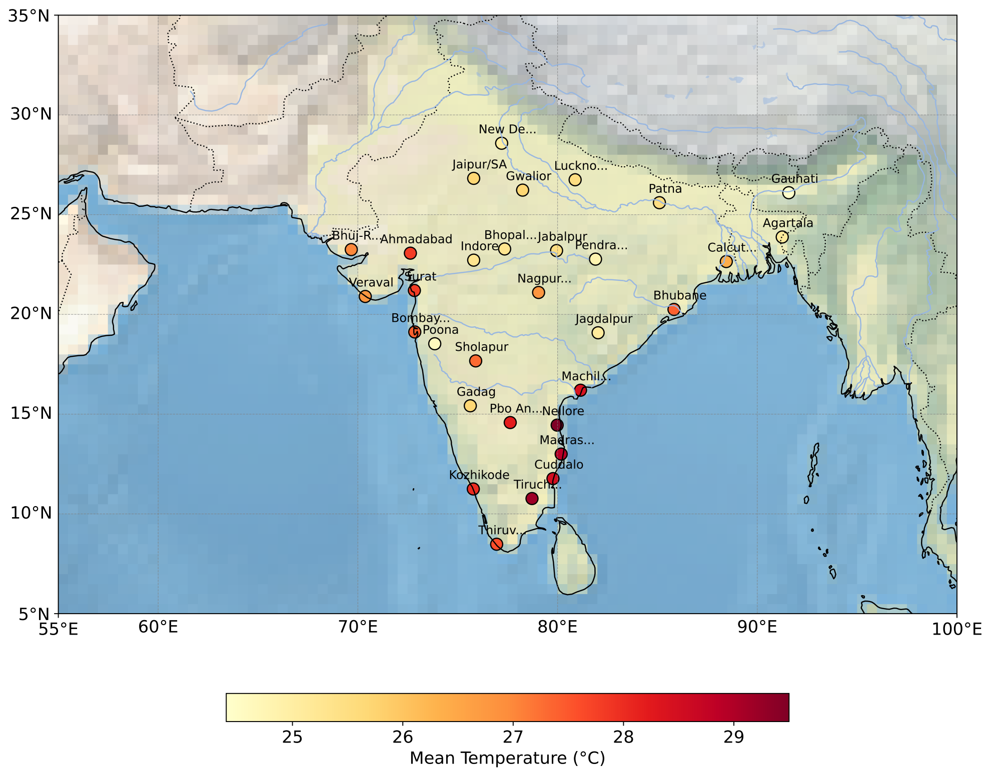

Figure 2: Geographical locations of the weather stations described in Table 1, along with a map displaying the mean temperature values at the selected stations within the domain spanning 55°E to 100°E and 5°N to 35°N. For clarity, station names are abbreviated to a maximum of seven characters, with additional characters replaced by dots (...). The mean temperature estimates are calculated as the average of daily minimum and maximum temperatures. Data was obtained from the Global Historical Climate Network – Daily (GHCND).

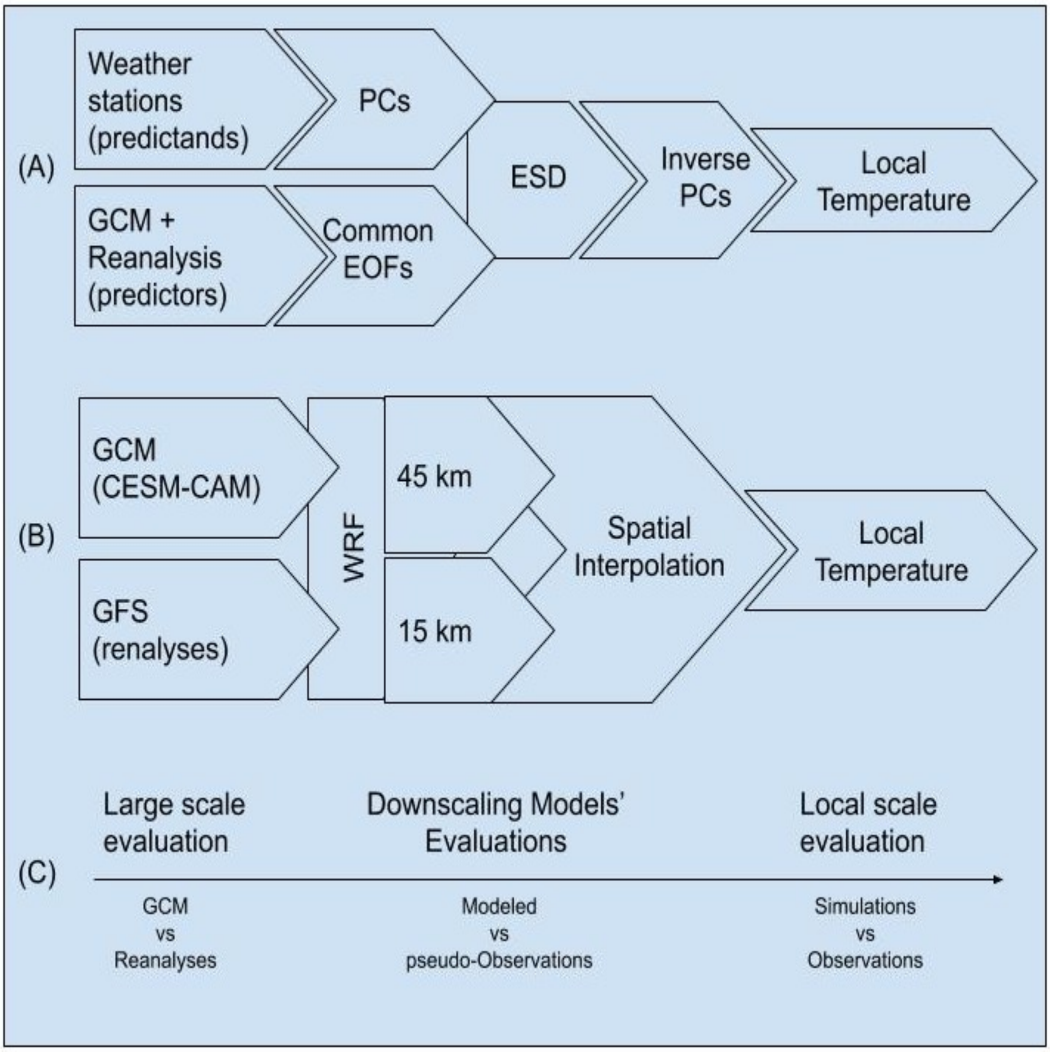

Figure 3: Workflow of the various simulations based on Empirical-Statistical Downscaling (A, ESD) and Dynamical Downscaling (B, WRF) along with different levels of evaluations (C). (Adapted from Mezgahni et al. 2019)

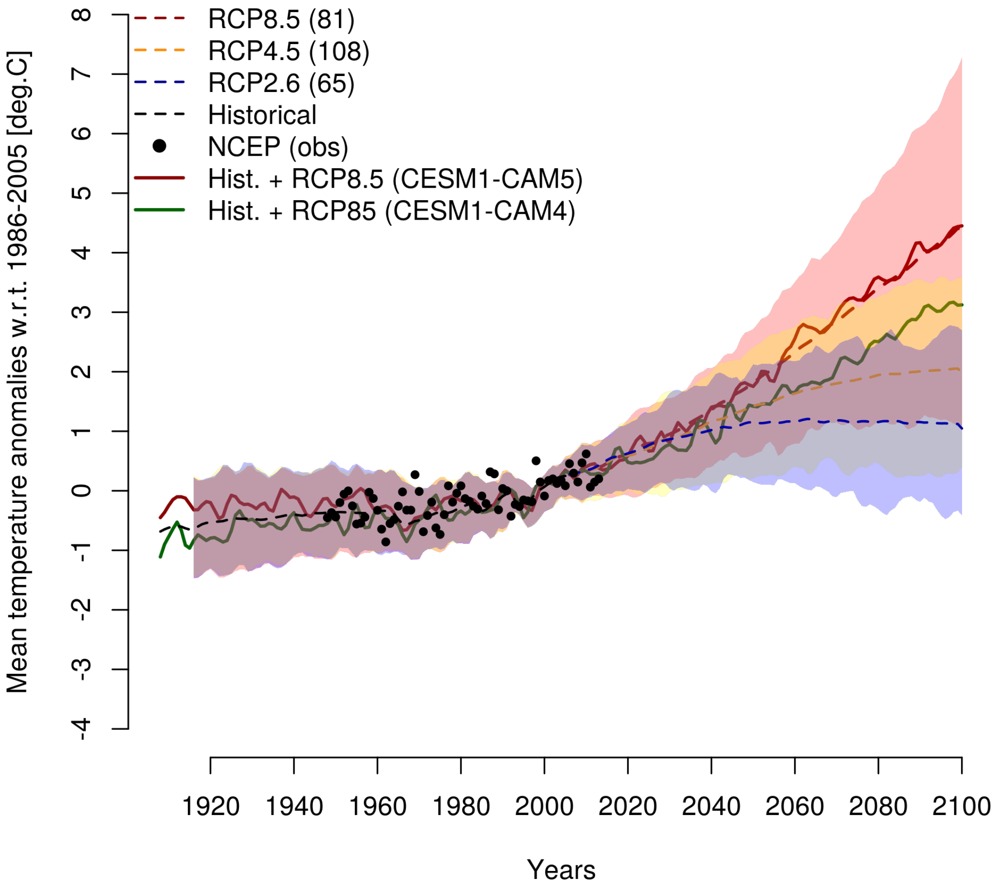

Figure 4: Regional estimates of annual mean temperature anomalies for the period 1920–2100 with regard to the based period 1986–2005 based on the full set of CMIP5 global climate model simulations for the historical (black) and assuming the three Radiative Concentration Pathways RCP2.6 (blue), RCP4.5 (orange), and RCP8.5 (red), respectively. Simulated temperature time series were first extracted, then area-averaged over the spatial domain extending from 55–100 East to 5–35 North as shown in Figure 2. The dashed lines and their corresponding envelopes represent multi-model ensembles' means and standard errors, respectively. The black dots correspond to temperature estimates from the NNRP taken as pseudo observation. The time series have been smoothed using a Spline filter. The envelopes show $0.7\times$ multi-model ensemble standard error($\sigma/\sqrt{N}$; where σ is the standard deviation and N is the total number of GCMs (displayed between brackets)). The green and deep pink lines highlight the CESM1-CAM5 and CESM1-CAM4 model simulations, respectively, for both historical and the RCP8.5 mitigation scenario.

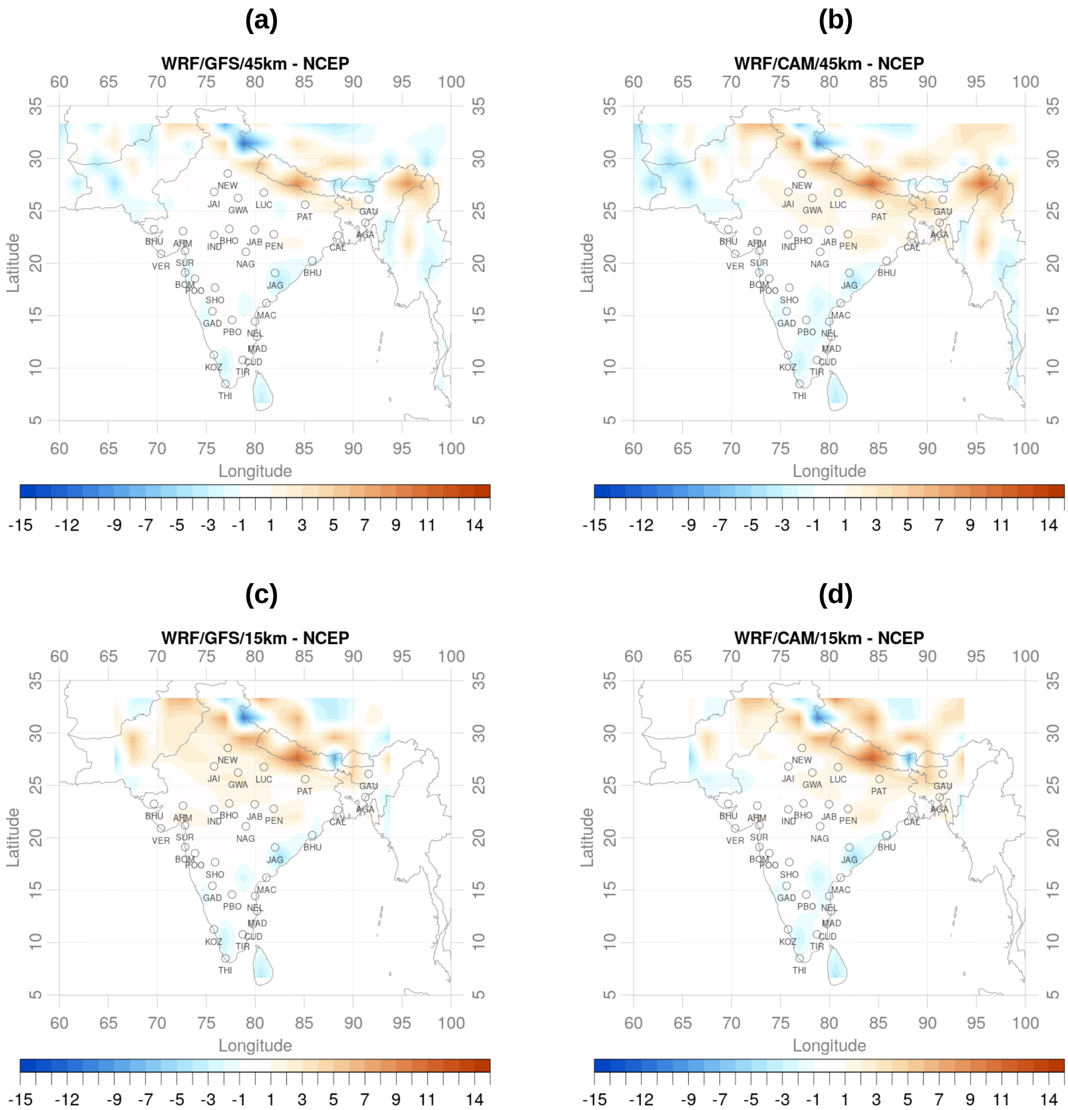

Figure 5: Biases in annual means of simulated temperature (in °C) by the WRF/NNRP (left) and WRF/CAM4 (right) model runs on a 45 km (top) and 15 km (bottom) grid resolutions, respectively, with regard to NNRP taken as reference. Model results were remapped to the NNRP grid resolution before the bias is computed. The circles show the geographical location of the selected weather stations along with their abbreviated names.

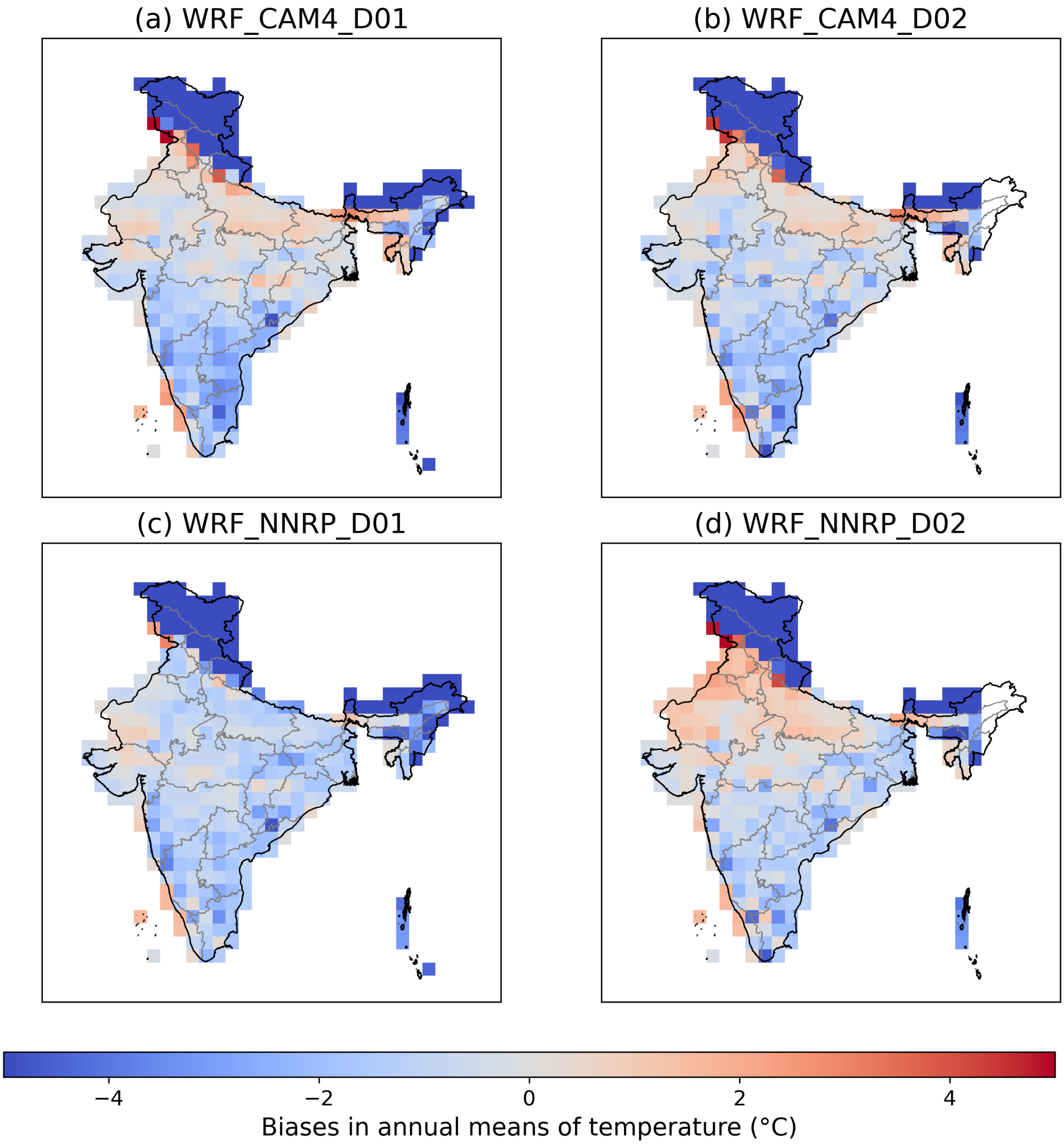

Figure 6: Biases in annual means of simulated temperature (in °C) by the WRF/CAM4 (top) and WRF/NNRP (bottom) model runs on a 45 km (left) and 15 km (right) grid resolutions, respectively, with regard to IMD data taken as reference. Model results were remapped to the IMD grid resolution (1 °× 1 °) before the bias is computed.

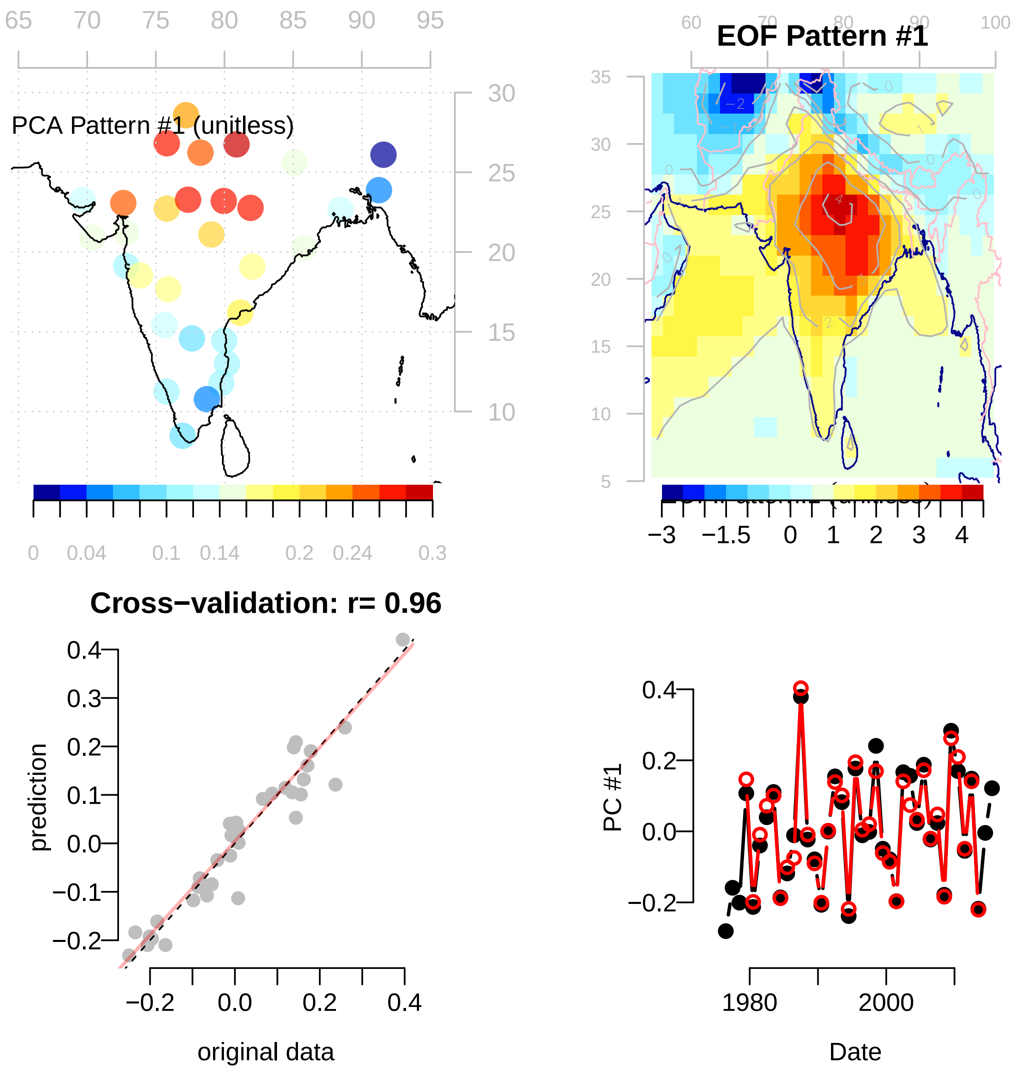

Figure 7: Example of an evaluation of the ESD method for JJA mean temperature. The inner plots correspond to the spatial pattern of the first principal component (PCA Pattern #1, top left panel) based on the observational network, the spatial pattern of the first Empirical-Orthogonal Function (EOF Pattern #1) based on the ERA-interim reanalyses data set (top right panel), cross-validation plot showing correlations between original data and predictions (bottom left panel), and time series of the fitted (red) versus original (black) PC #1 (bottom right panel). The color bars in the top sub panels are dimensionless and indicate high (red palette) and low (blue palette) systems of the spatial pattern.

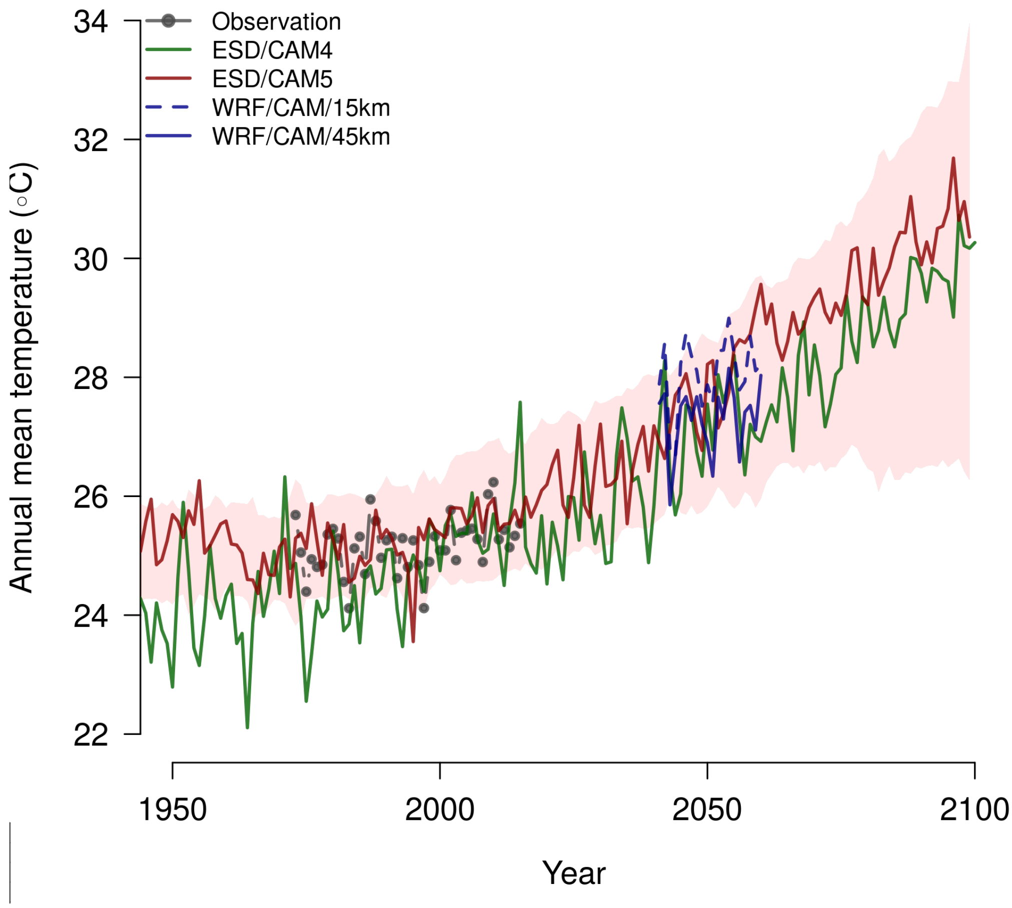

Figure 8: Downscaled temperature values at 'New Delhi/S' weather station. Annual mean values were derived from ESD simulation (red) for the period spanning from 1940 to 2100, the WRF/NNRP (green) for the period 1986–2005 and WRF/CESM-CAM4 (blue) for the period 2041–2060 assuming the high RCP8.5 emission scenario. The WRF simulations were bi-linearly interpolated to the 'New Delhi/S' weather station for the low (45 km; dashed lines) and high (15 km; continuous lines) spatial domains, respectively. The grey dotted line shows observations and the envelope indicates the 95th confidence interval ($\sigma_e = 1.96 \times \sigma$, where σ is the standard derivation of ESD-based CMIP5 multi-model ensemble).

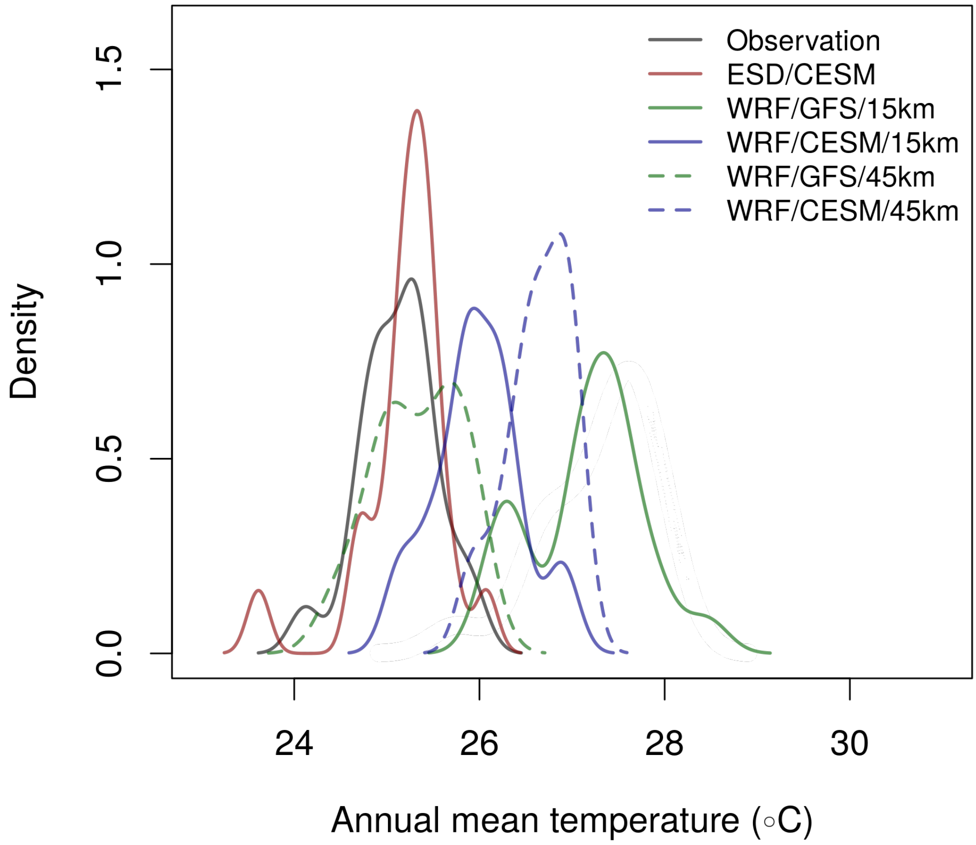

Figure 9: Empirical density function of annual mean temperature at 'New Delhi/S' weather station based on various experiments/simulations over the control time period 1986–2005. Annual mean values are estimated from the weather station (black) and interpolated from ESD driven by the CESM-CAM4 simulation (red) and for the WRF simulations driven by NNRP (green) and CESM-CAM5 (blue) and considering the two spatial domains with 45km and 15km (dashed lines) grid resolutions, respectively.

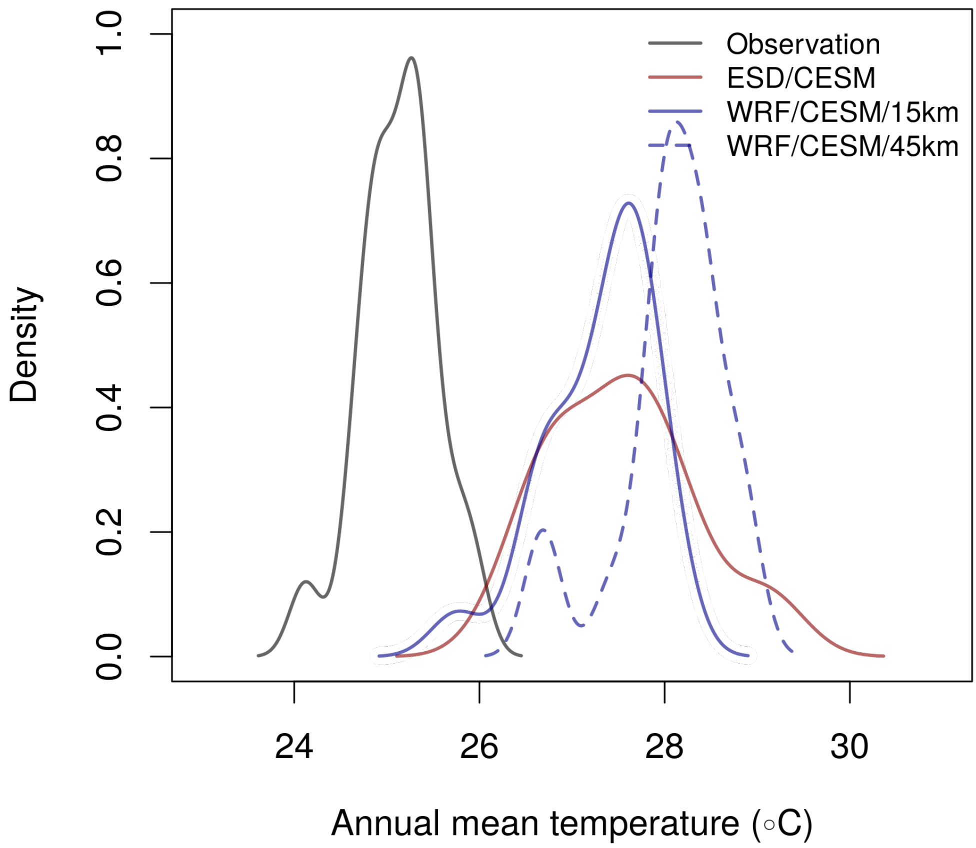

Figure 10: Density function of future mean temperature values at 'New Delhi/S' weather station based on various experiments/simulations over the period 2041–2060. Same caption details as in Figure 9.

Table 1: **General characteristics of selected temperature weather stations in India**. These are the location name, the geographical coordinates in terms of longitude (Degrees East) and latitude (Degrees North), the elevation above sea level (m) at the weather station as well as in WRF/45km and WRF/15km runs, the percentage of missing daily values in the period 1986–2005, and the estimated mean daily values (°C) calculated as the average between the daily minimum and maximum recorded values. The temperature data and meta data were obtained from the Global Historical Climate Network – Daily (GHCN-D).

ID	Location Name	Lon. (°E)	Lat. (°N)	Alt. (m)	Alt. (m)	Alt. (m)	Missing (%)	Mean (°C)
				Station	WRF45km	WRF15km		
1	Pbo Anantapur	77.63	14.58	364	414	362	30	28.2
2	Machilipatnam	81.15	16.20	3	4	3	32	28.4
3	Nellore	79.98	14.45	20	24	16	32	29.5
4	Gauhati	91.58	26.10	54	166	113	28	24.4
5	Patna	85.10	25.60	60	50	47	32	25.5
6	Ahmadabad	72.63	23.07	55	54	57	33	27.8
7	Veraval	70.37	20.90	8	33	17	34	26.8
8	Bhuj-Rudramata	69.67	23.25	80	66	145	31	27.0
9	Surat	72.83	21.20	12	14	11	34	27.8
10	Gadag	75.63	15.42	650	590	648	39	25.7
11	Kozhikode	75.78	11.25	5	40	11	42	28.0
12	Thiruvananthapuram	76.95	08.48	64	54	18	26	27.6
13	Jagdalpur	82.03	19.08	553	566	560	42	25.1
14	Pendra Road	81.90	22.77	625	545	621	45	24.8
15	Gwalior	78.25	26.23	207	195	202	44	25.7
16	Indore	75.80	22.72	567	492	559	33	25.3
17	Jabalpur	79.95	23.20	393	467	393	43	25.5
18	Bhopal/Bairagarh	77.35	23.28	523	474	510	29	25.3
19	Bombay/Santacruz	72.85	19.12	14	39	12	40	27.4
20	Nagpur Sonega	79.05	21.10	310	326	300	30	26.8
21	Poona	73.85	18.53	559	665	640	23	24.6
22	Sholapur	75.90	17.67	479	482	466	24	27.3
23	Bhubane	85.83	20.25	46	35	43	29	27.4
24	Jaipur/SA	75.80	26.82	390	365	365	52	25.7
25	Cuddalo	79.77	11.77	12	18	17	33	28.5
26	Madras/Minambakkam	80.18	13.00	16	19	17	35	28.9
27	Tiruchchirapalli	78.72	10.77	88	161	82	37	29.2
28	Agartala	91.25	23.88	16	32	21	35	25.1
29	New Delhi/S	77.20	28.58	216	208	220	23	25.0
30	Lucknow/Amausi	80.88	26.75	128	120	122	49	25.5
31	Calcutta/Dum	88.45	22.65	6	7	11	40	26.4

Table 2: Description of the simulations used in this study.

Acronym	Scenario	GCM	RCM	Description
WRF/NNRP	RCP8.5	NNRP	WRF	WRF model forced by the NNRP and interpolated to station.
WRF/CAM4	RCP8.5	CESM1-CAM4	WRF	WRF model forced by the CESM1-CAM4 and interpolated to station.
ESD/CAM4	RCP8.5	CESM1-CAM4	N/A	ESD forced by the CESM1-CAM4 directly to stations.
ESD/CMIP5	RCP8.5	CMIP5-Ensemble	N/A	ESD forced by the full CMIP5/GCM ensemble – including CESM1-CAM5 – directly to stations.

WRF, Weather Research Forecast

NNRP, NCEP/NCAR Reanalysis Product

CESM1-CAM4/5, Community Earth System version 1 - Community Atmosphere Model version 4/5

N/A, not applicable

Table 3: Annual and seasonal mean temperature (°C) as estimated from various reanalyses data sets such as NNRP, ERAINT and ERA5, and MERRA and modeled by the CESM1-CAM5 model. Mean values were calculated using the average over the domain spanning from 55 to 100 degrees east and from 5 to 35 degrees north encompassing parts of the Arabian sea, the bay of Bengal and parts of the Indian ocean (land + sea, and not only land) and averaged over the time period 1986–2005. The Ens. SD and Mean correspond to the standard deviation and mean of the multi-reanalyses ensemble, while, the Bias in the last row shows annual and seasonal deviations of CESM1-CAM4 model from the multi-reanalyses ensemble mean.

	Annual	DJF	MAM	JJA	SON
Reanalyses					
- NNRP	22.1	17.5	23.7	25.6	21.8
- ERAINT	22.8	18.2	24.0	26.2	22.9
- ERA5	22.4	17.8	23.6	25.8	22.5
- MERRA	23.1	18.5	24.6	26.4	23.1
Ens. Mean	22.6	18.0	24.0	26.0	22.6
Ens. SD	0.4	0.4	0.5	0.4	0.5
Model-Run					
- CESM1-CAM4	22.8	17.4	23.9	26.7	23.1
Bias	0.2	-0.6	-0.1	0.7	0.6

DJF, December-January-February season; MAM, March-April-May season; JJA, June-July-August season; SON, September-October-November season

Table 4: Cross-validation based on the top five leading principal components. The values correspond to Spearman correlations calculated based on original and estimated time series for each principal component derived from each of the reanalyses ERAINT, ERA5, MERRA, and NNRP, respectively.

Rea.	Sea.	PC1	PC2	PC3	PC4	PC5
ERAINT	DJF	0.96	0.74	0.71	0.64	0.39
	MAM	0.89	0.85	0.65	-0.29	0.79
	JJA	0.96	0.82	0.81	-0.28	0.27
	SON	0.77	0.69	0.48	0.29	0.33
ERA5	DJF	0.84	0.67	0.50	0.30	-0.11
	MAM	0.52	0.59	0.69	-0.03	0.79
	JJA	0.89	0.61	0.79	0.03	0.21
	SON	0.94	0.67	0.10	0.27	0.00
MERRA	DJF	0.77	0.60	0.43	0.64	0.06
	MAM	0.88	0.80	0.48	-0.26	0.39
	JJA	0.81	0.60	0.63	-0.08	0.25
	SON	0.87	0.65	0.25	0.62	-0.02
NNRP	DJF	0.79	0.54	0.63	0.46	-0.44
	MAM	0.48	0.29	0.41	-0.15	0.31
	JJA	0.82	0.13	0.58	0.40	0.17
	SON	0.68	0.39	0.38	0.34	-0.14

Rea., Reanalyses

Sea., Season

PC, Principal Component

DJF, December-January-February season; MAM, March-April-May season; JJA, June-July-August season; SON, September-October-November season

Table 5: **Biases (°C) of annual mean temperatures under RCP8.5 scenario** from WRF and ESD models driven by NNRP, CESM1-CAM4, and CESM1-CAM5. Biases are calculated as deviations from observations averaged over 1986–2005. The last two rows show the spatial average (Average) and variation (Standard Deviation) across the observational network.

Experiment	WRF/NNRP		WRF/CAM4		ESD	
Location	45 km	15 km	45 km	15 km	CAM4	CAM5
Pbo Anantapur	-2.2	-1.5	-3.2	-2.3	-0.5	-0.2
Machilipatnam	-1.7	-1.3	-2.3	-1.6	-0.2	0.1
Nellore	-1.9	-1.6	-2.8	-2.2	-0.1	0.1
Gauhati	-3.0	-2.3	-1.5	-1.1	-0.2	0.1
Patna	-0.6	1.3	0.9	1.9	-0.2	0.1
Ahmadabad	-1.0	1.3	-1.0	0.5	-0.7	-0.3
Veraval	-1.1	-0.3	-1.0	-0.5	-0.3	0.1
Bhuj-Rudramata	-0.3	-1.3	-0.5	-1.9	0.0	0.2
Surat	-1.4	0.8	-1.7	0.3	-0.5	-0.2
Gadag	-0.7	-1.4	-1.1	-1.8	-0.3	-0.1
Kozhikode	-2.0	-2.1	-1.3	-1.3	-0.1	0.0
Thiruvananthapuram	-0.9	-1.1	-0.9	-0.9	-0.1	0.0
Jagdalpur	-1.1	-0.8	-1.0	-0.7	-0.3	-0.1
Pendra Road	-0.3	-0.5	0.9	-0.4	-0.1	0.2
Gwalior	-0.4	1.3	0.8	0.5	-0.3	-0.1
Indore	0.4	0.5	0.4	-0.3	-0.5	-0.3
Jabalpur	-1.8	-0.0	-1.1	-0.4	-0.3	0.1
Bhopal/Bairagarh	-0.1	-0.0	0.2	-0.7	-0.3	-0.0
Bombay/Santacruz	-1.4	0.6	-1.3	0.4	-0.2	-0.1
Nagpur Sonega	-0.6	-0.1	-0.2	-0.4	-0.3	0.0
Poona	-2.4	-0.9	-2.2	-0.8	-0.2	0.1
Sholapur	-1.3	-0.8	-1.7	-1.2	-0.2	0.1
Bhubane	-1.2	-1.2	-1.0	-1.2	-0.3	0.1
Jaipur/SA	-0.8	0.9	0.1	-0.2	-0.5	-0.1
Cuddalo	-1.1	-1.0	-2.0	-1.6	-0.2	-0.1
Madras/Minambakkam	-1.7	-1.3	-2.5	-2.0	-0.2	0.0
Tiruchchirapalli	-2.3	-1.5	-3.4	-2.3	-0.2	0.0
Agartala	-1.8	-1.2	-0.1	-0.2	-0.1	0.1
New Delhi/S	0.4	3.6	1.7	2.6	-0.2	0.1
Lucknow/Amausi	-0.9	1.7	0.6	1.3	-0.3	-0.1
Calcutta/Dum	-1.3	-1.0	-0.1	-0.3	-0.2	0.0
– Average	-1.2	-0.4	-0.9	-0.6	-0.3	0.0
– Standard Deviation	0.8	1.3	1.3	1.2	0.1	0.1

Table 6a: **Biases (°C) of seasonal mean temperatures for DJF and MAM seasons under RCP8.5 scenario** from WRF and ESD models driven by NNRP, CESM1-CAM4, and CESM1-CAM5. Biases are calculated as deviations from observations averaged over 1986–2005. The last two rows show the spatial average (Average) and variation (Standard Deviation) across the observational network.

Location – Season	DJF						MAM					
	WRF/NNRP		WRF/CAM4		ESD		WRF/NNRP		WRF/CAM4		ESD	
	45km	15km	45km	15km	CAM4	CAM5	45km	15km	45km	15km	CAM4	CAM5
Pbo Anantapur	-2.8	-4.4	-2	-3.8	-0.5	0	-1.9	-1.7	-2.8	-3	-0.5	-0.2
Machilipatnam	-2.9	-2.8	-2.2	-1.9	-0.1	0.4	-0.9	-1.6	-2.8	-3.6	-0.1	0
Nellore	-2.9	-3.1	-1.9	-2.2	0	0.3	-1.7	-2.7	-3.5	-4.7	0	0.1
Gauhati	-4.5	-2.3	-3.1	-2.2	-0.5	0.2	-1.7	-1.1	0.5	0.8	0	0.3
Patna	-1.1	0.4	1.6	1.1	-0.4	0.3	-0.3	1.8	1.8	3	0.2	0.2
Ahmadabad	-1.9	-2.2	1.7	-0.1	-0.8	0.1	-1.4	0.3	-1.3	0.5	-0.8	-0.1
Veraval	-1.4	-1.5	0.1	-0.6	-0.8	0.4	-0.8	-0.3	-0.3	-0.4	0.1	0.2
Bhuj-Rudramata	0.2	0.4	-0.4	-1.6	-0.2	0.5	-1.3	-2.4	-1.1	-2.4	0	0.2
Surat	-1.4	-2.5	1.4	-0.1	-0.5	0	-1	1	-1.4	0.7	-0.4	0
Gadag	-0.9	-2.4	-1.3	-3.2	-0.2	0.3	-0.2	-1.4	-0.7	-1.8	-0.3	-0.1
Kozhikode	-1.7	-2	-2.1	-1.6	0.1	0.1	-2.6	-3	-2.2	-2.4	-0.2	0.1
Thiruvananthapuram	-1.4	-1.8	-1.6	-1.6	-0.1	0	-1.2	-1.7	-1.5	-1.8	-0.1	0
Jagdalpur	-1.2	-1.2	-1.4	-1.3	-0.2	0.4	-0.5	-0.6	-1.5	-1.5	-0.1	-0.1
Pendra Road	-1.2	-0.7	-1.7	-2.3	-0.4	0	0.5	0.3	2	0.1	0.4	0.1
Gwalior	-1.2	0.2	0.4	-0.8	-0.5	0.3	-0.1	1.5	1.3	0.9	0.2	0.2
Indore	0.3	-1.5	0.4	-1.6	-0.8	0	0.9	0.3	1.3	0	-0.6	-0.1
Jabalpur	-1.8	-2.2	-0.4	-1.6	-0.4	0.2	-1	0.5	-0.1	-0.1	-0.1	0
Bhopal/Bairagarh	-0.7	-1.6	-0.9	-2.5	-0.6	0.3	0.4	0.1	1	-0.4	-0.3	0.1
Bombay/Santacruz	-1	-1.4	1.3	0.9	-0.6	0	-1.3	0.5	-1.3	0.1	0.2	0.2
Nagpur Sonega	-1	-1.6	-1.1	-2.1	-0.6	0.3	0.4	0.6	0.7	0.1	-0.1	0.1
Poona	-1.1	-2.2	0.4	-0.7	-0.4	0.5	-2.1	-0.6	-1.8	-0.3	0.1	0.3
Sholapur	-1.8	-3	-1.1	-2.8	0.1	0.5	-1	-0.5	-0.9	-0.9	-0.1	0.2
Bhubane	-2	-1.1	-1.9	-1.9	-0.4	0.5	-1.4	-1.8	-2.4	-2.6	-0.4	0.1
Jaipur/SA	-2	-1	-0.2	-1.7	-0.7	0.2	-0.6	0.7	0.4	0	-0.5	0.2
Cuddalo	-1.4	-1.9	-0.7	-0.9	-0.2	0	-1	-1.9	-2.5	-3.6	-0.2	-0.1
Madras/Minambakkam	-2.2	-2.4	-0.9	-1.3	-0.2	0.1	-1.8	-2.6	-3.2	-4.3	0	0
Tiruchchirapalli	-2.5	-3.6	-1.8	-2.6	-0.2	0	-2.2	-2.2	-3.9	-3.8	-0.1	0
Agartala	-2.7	0	-1.4	-0.6	-0.2	0.3	-0.8	-0.8	0.2	0.2	0.2	0.4
New Delhi/S	-0.5	1.4	3	1.2	-0.3	0.3	0.1	3.7	1.7	3	-0.1	0.4
Lucknow/Amausi	-1.9	0	1.2	-0.1	-0.2	-0.2	-0.8	2.1	1.2	2	-0.5	0
Calcutta/Dum	-1.8	0.1	-0.7	-0.5	-0.3	0.1	-0.5	-0.5	0.1	0.1	-0.1	0.2
– Average	-1.6	-1.5	-0.6	-1.3	-0.4	0.2	-0.9	-0.4	-0.7	-0.8	-0.1	0.1
– Standard Deviation	1	1.3	1.4	1.2	0.2	0.2	0.8	1.6	1.7	2	0.3	0.1

Table 6b: **Biases (°C) of seasonal mean temperatures for JJA and SON seasons under RCP8.5 scenario** from WRF and ESD models driven by NNRP, CESM1-CAM4, and CESM1-CAM5. Biases are calculated as deviations from observations averaged over 1986–2005. The last two rows show the spatial average (Average) and variation (Standard Deviation) across the observational network.

Location – Season	JJA						SON					
	WRF/NNRP		WRF/CAM4		ESD		WRF/NNRP		WRF/CAM4		ESD	
	45km	15km	45km	15km	CAM4	CAM5	45km	15km	45km	15km	CAM4	CAM5
Pbo Anantapur	-1.8	-1	-2.7	-0.9	-0.3	0.2	-2.7	-1.4	-3.2	-1.7	-0.6	-0.6
Machilipatnam	-0.6	-0.2	-1.3	0	-0.2	0.3	-2.8	-1.5	-2.3	-1	-0.2	-0.2
Nellore	-0.9	-0.8	-2.5	-0.9	-0.1	0.3	-2.2	-1.1	-2.3	-1.3	-0.2	-0.1
Gauhati	-1.6	-1.7	-1.6	-1.2	0	0.1	-4.7	-3.5	-3	-2.2	-0.2	-0.1
Patna	1.5	1.6	1.5	2.2	-0.1	0.4	-2.9	-0.3	-0.6	0.9	-0.4	-0.2
Ahmadabad	0.3	1.2	0.3	0.6	-0.2	-0.2	-1.2	1.8	-1	0.9	-0.8	-0.9
Veraval	-0.8	-0.6	-1	-0.8	-0.2	0	-1.8	-0.6	-1.6	-0.5	-0.5	-0.5
Bhuj-Rudramata	-0.3	-2	-1.1	-2.5	-0.1	-0.2	-0.5	-1.1	-0.7	-1.5	0.2	0
Surat	-1.2	0.1	-1	-0.2	-0.2	-0.2	-2	0.6	-2.1	0.4	-0.8	-0.7
Gadag	-0.5	-1.2	-0.3	-0.7	-0.3	0	-1.1	-1.7	-1.2	-1.7	-0.5	-0.5
Kozhikode	-1.4	-1.2	0	0	-0.2	0.1	-2.2	-2.2	-1.2	-1.2	-0.2	-0.1
Thiruvananthapuram	-0.3	-0.3	0.1	0.2	-0.1	0.2	-0.8	-1	-0.5	-0.5	-0.1	0
Jagdalpur	-0.3	0.3	0.2	0.8	-0.2	0	-2.6	-1.9	-1.7	-1.1	-0.7	-0.6
Pendra Road	1.1	0.9	2.1	1	-0.3	0.3	-2.2	-2	-0.3	-1.2	-0.3	0
Gwalior	1.6	2.6	1.6	1.7	0	0	-2.3	0.3	-0.6	-0.3	-0.8	-0.8
Indore	1	1	1.9	0.6	-0.1	-0.2	-0.6	0	-0.6	-0.6	-0.7	-0.7
Jabalpur	-0.7	1.3	0.2	0.7	-0.1	0.4	-3.9	-1.7	-2.5	-1.2	-0.4	-0.3
Bhopal/Bairagarh	1	1.4	2	0.9	0.1	0.1	-1.5	-1.1	-0.9	-1.3	-0.5	-0.6
Bombay/Santacruz	-1.4	0	-1.1	-0.3	-0.2	-0.1	-1.9	0.4	-1.6	0.6	-0.4	-0.4
Nagpur Sonega	0	1.2	1	1.1	-0.2	0.1	-2.2	-1.6	-1.3	-1	-0.4	-0.4
Poona	-3.4	-2	-2.4	-1.4	-0.1	0.2	-3	-1.4	-2.4	-0.8	-0.6	-0.6
Sholapur	-0.9	-0.4	-0.9	-0.1	-0.2	0.5	-1.6	-1.4	-2.1	-1.4	-0.5	-0.7
Bhubane	-0.1	0.1	0.1	0.3	-0.2	0.2	-1.8	-1.5	-0.8	-0.9	-0.4	-0.4
Jaipur/SA	1.3	2.4	1.5	1.3	0.1	0	-2.4	0.3	-1	-0.9	-0.8	-0.7
Cuddalo	-0.9	-1	-2.4	-1.5	-0.3	0	-1.2	-0.5	-1.4	-0.7	-0.3	-0.2
Madras/Minambakkam	-1.1	-1	-2.5	-1.4	-0.3	0.2	-1.9	-0.8	-2	-1	-0.2	-0.1
Tiruchchirapalli	-2.2	-1.4	-3.6	-1.7	0	0.3	-2.2	-1	-2.8	-1.4	-0.3	-0.3
Agartala	-0.7	-0.5	0.3	0.3	0	0.3	-3.2	-2.2	-1.3	-1	-0.5	-0.5
New Delhi/S	2.5	4.3	2.6	3.7	0	0.3	-1	2.8	0.6	1.9	-0.4	-0.4
Lucknow/Amausi	1.6	2.8	1.4	2.4	-0.3	0.1	-3.1	0.2	-0.8	0.2	-0.4	-0.2
Calcutta/Dum	-0.5	-1	0.2	-0.3	-0.1	0	-3	-2.1	-1.2	-0.7	-0.1	-0.1
– Average	-0.3	0.2	-0.2	0.1	-0.1	0.1	-2.1	-0.9	-1.4	-0.7	-0.4	-0.4
– Standard Deviation	1.3	1.5	1.7	1.3	0.1	0.2	0.9	1.3	0.9	0.9	0.2	0.3

Table 7: **WRF future changes in seasonal and annual means of estimated daily mean temperature (°C) at the selected weather stations across India and assuming the high emission scenario RCP8.5 by 2041–2060**. Absolute temperature changes are defined as deviations between the future (2041–2060) and historical (1986–2005) WRF simulations driven by the global climate model and for the two 45 km and 15 km grid resolutions, respectively. The last two rows in the table show the spatial average and standard deviation over all sites.

	WRF/45km					WRF/15 km				
Location | Season	DJF	MAM	JJA	SON	ANN	DJF	MAM	JJA	SON	ANN
Pbo Anantapur	1.3	1.6	1.3	1.2	1.3	1.2	1.3	1.3	1.3	1.3
Machilipatnam	1.1	1.4	1.3	1.2	1.2	1.0	1.7	1.3	0.9	1.2
Nellore	1.1	1.4	1.4	1.2	1.2	1.0	1.7	1.5	1.2	1.3
Gauhati	1.7	1.5	1.4	1.5	1.5	1.9	1.6	1.5	1.3	1.6
Patna	1.8	1.6	1.4	1.5	1.6	1.7	1.7	1.4	1.1	1.5
Ahmadabad	2.3	1.4	0.9	1.5	1.5	1.6	1.1	1.1	1.1	1.2
Veraval	2.0	1.1	1.0	1.4	1.3	1.6	1.1	1.1	1.3	1.3
Bhuj-Rudramata	2.3	1.2	1.0	1.6	1.5	1.4	1.1	1.1	1.2	1.2
Surat	2.1	1.2	0.9	1.4	1.4	1.7	1.0	1.1	1.2	1.2
Gadag	1.4	1.4	1.1	1.1	1.2	1.2	1.1	1.1	1.3	1.2
Kozhikode	1.1	1.0	1.2	1.4	1.2	1.1	1.0	1.2	1.4	1.2
Thiruvananthapuram	1.1	1.0	1.2	1.4	1.1	1.1	1.0	1.2	1.4	1.2
Jagdalpur	1.4	1.6	1.3	1.3	1.3	1.3	1.8	1.4	1.1	1.3
Pendra Road	1.9	1.7	1.3	1.3	1.5	2.1	1.7	1.4	1.2	1.6
Gwalior	2.0	1.5	1.0	1.4	1.5	1.7	1.4	1.4	1.0	1.3
Indore	2.2	1.6	0.7	1.4	1.5	1.9	1.2	1.0	1.1	1.3
Jabalpur	2.1	1.7	1.1	1.4	1.5	2.0	1.5	1.4	1.1	1.5
Bhopal/Bairagarh	2.2	1.6	0.8	1.5	1.5	1.9	1.4	1.1	1.1	1.3
Bombay/Santacruz	1.6	1.1	0.9	1.2	1.2	1.5	1.0	1.1	1.3	1.2
Nagpur Sonega	1.9	1.7	1.0	1.4	1.5	1.9	1.5	1.1	1.1	1.4
Poona	1.7	1.4	1.0	1.2	1.3	1.4	1.0	1.1	1.2	1.2
Sholapur	1.5	1.5	1.0	1.1	1.2	1.3	1.1	1.0	1.2	1.2
Bhubane	1.4	1.4	1.3	1.3	1.3	1.3	1.8	1.4	1.1	1.3
Jaipur/SA	2.0	1.5	0.9	1.4	1.5	1.7	1.3	1.3	1.2	1.3
Cuddalo	1.0	1.3	1.4	1.2	1.2	1.1	1.4	1.5	1.3	1.3
Madras/Minambakkam	1.0	1.4	1.3	1.2	1.2	1.1	1.5	1.6	1.2	1.3
Tiruchchirapalli	1.1	1.4	1.5	1.2	1.3	1.2	1.1	1.3	1.4	1.2
Agartala	1.5	1.2	1.2	1.3	1.3	1.8	1.5	1.4	1.2	1.5
New Delhi/S	1.8	1.5	1.2	1.4	1.5	1.6	1.4	1.2	1.1	1.3
Lucknow/Amausi	1.8	1.5	1.3	1.4	1.5	1.6	1.5	1.3	1.0	1.3
Calcutta/Dum	1.7	1.4	1.3	1.3	1.4	1.7	1.7	1.3	1.2	1.5
– Average	1.6	1.4	1.1	1.3	1.4	1.5	1.4	1.3	1.2	1.3
– Standard Deviation	0.4	0.2	0.2	0.1	0.1	0.3	0.3	0.2	0.1	0.1

Table 8: **ESD future changes in seasonal and annual means of daily mean temperature (°C) at the selected weather stations across India and assuming the high emission scenario RCP8.5**. Absolute temperature changes were derived from the empirical–statistical downscaling (ESD) results driven by the CESM1-CAM4 global climate model. Values were estimated as future deviations from the historical base-period 1986–2005 for two horizons 2041–2060 and 2081–2100, respectively. The last two rows in the table show the spatial average and standard deviation over all sites.

	ESD changes by 2041–2060					ESD changes by 2081–2100				
Location | Season	DJF	MAM	JJA	SON	ANN	DJF	MAM	JJA	SON	ANN
Pbo Anantapur	1.3	1.2	1.0	1.1	1.1	2.6	2.0	2.0	2.3	2.2
Machilipatnam	1.5	0.3	2.3	1.5	1.4	3.0	0.6	4.4	3.2	2.8
Nellore	1.0	0.4	1.2	1.0	0.9	2.0	0.6	2.2	2.0	1.7
Gauhati	1.9	0.6	0.3	1.8	1.1	4.2	1.1	0.5	3.4	2.3
Patna	1.3	1.1	0.9	2.4	1.4	2.7	1.8	1.9	4.6	2.8
Ahmadabad	2.4	1.8	1.0	4.0	2.3	5.2	3.2	2.0	8.1	4.6
Veraval	2.8	0.1	0.2	3.2	1.6	6.1	0.4	0.6	6.5	3.4
Bhuj-Rudramata	1.7	1.2	1.4	2.3	1.7	3.8	2.7	2.8	4.5	3.4
Surat	1.1	1.0	0.5	0.9	0.9	2.4	1.8	1.2	1.9	1.8
Gadag	1.6	1.5	0.7	1.4	1.3	3.2	2.7	1.5	3.1	2.6
Kozhikode	0.6	0.9	0.9	0.8	0.8	1.3	1.9	1.7	1.8	1.7
Thiruvananthapuram	0.5	0.7	0.9	0.4	0.6	0.9	1.4	1.8	0.8	1.2
Jagdalpur	2.6	1.3	1.4	2.6	2.0	5.5	2.1	3.1	5.3	4.0
Pendra Road	2.1	0.9	1.3	0.1	1.1	4.4	1.7	2.8	0.3	2.3
Gwalior	2.3	3.2	0.0	4.9	2.6	5.0	6.4	0.1	9.8	5.3
Indore	2.5	1.2	-0.3	2.8	1.6	5.4	2.0	-0.2	6.0	3.3
Jabalpur	2.9	1.6	0.4	2.1	1.7	6.1	3.0	1.3	4.4	3.7
Bhopal/Bairagarh	2.7	1.3	-0.3	3.7	1.8	5.8	2.3	-0.1	7.5	3.9
Bombay/Santacruz	2.0	0.9	0.5	1.9	1.3	4.4	2.0	1.2	4.1	2.9
Nagpur Sonega	3.6	2.4	0.4	3.1	2.4	7.6	4.0	1.3	6.2	4.8
Poona	3.1	1.4	0.8	2.9	2.1	6.5	3.0	2.0	5.8	4.3
Sholapur	2.7	1.9	1.2	3.0	2.2	5.7	3.8	2.5	6.1	4.5
Bhubane	2.7	1.3	0.3	2.3	1.6	5.8	2.2	0.6	4.8	3.3
Jaipur/SA	2.8	0.5	0.3	3.4	1.8	6.0	1.3	0.5	7.2	3.8
Cuddalo	0.8	0.2	1.1	0.9	0.8	1.6	0.1	2.0	2.0	1.4
Madras/Minambakkam	1.3	0.3	1.0	1.0	0.9	2.7	0.5	1.7	1.8	1.7
Tiruchchirapalli	0.9	1.1	1.3	1.3	1.1	1.9	2.1	2.3	2.7	2.2
Agartala	1.5	1.1	0.2	3.7	1.6	3.4	1.9	0.5	7.3	3.3
New Delhi/S	1.5	2.2	1.1	3.4	2.1	3.3	4.4	2.1	6.6	4.1
Lucknow/Amausi	1.4	1.8	0.5	1.7	1.4	3.0	3.2	1.3	3.7	2.8
Calcutta/Dum	1.2	1.5	0.6	1.5	1.2	2.5	2.7	1.1	3.0	2.3
– Average	1.9	1.2	0.7	2.2	1.5	4.0	2.2	1.6	4.4	3.0
– Standard Deviation	0.8	0.7	0.6	1.2	0.5	1.8	1.3	1.0	2.3	1.1

Table 9: Comparison of WRF (Dynamical Downscaling) and ESD (Empirical-Statistical Downscaling) Temperature Projections over India

Aspect	WRF (Dynamical Downscaling)	ESD (Empirical-Statistical Downscaling)
Driving Data	Driven by NNRP reanalysis and CESM1-CAM4 outputs	Trained on ERA-Interim (ERAINT) reanalysis data
Model	Weather Research and Forecasting (WRF) model	Empirical-statistical downscaling method
Horizontal Resolution	Performed at 45 km and 15 km resolutions	Station-level projections at meteorological stations
Historical Skill	Some discrepancies in simulating historical temperatures at individual sites	Statistical training on ERA-Interim offers reliable station-scale projections
Projected Temperature Increases	Generally projects lower warming compared to ESD	Projects larger temperature increases across annual and seasonal timescales
Impact of Resolution	Increasing resolution from 45 km to 15 km had negligible impact on projected warming (differences < 0.1 °C)	Not applicable (station scale projections)
Local Cooling Trends	Small cooling trends during monsoon at a few stations (e.g., Indore, Bhopal) also noted	Similar cooling trends noted in monsoon season at select high-elevation stations
Warming by 2050	Approximately 1.5 °C warming projected over India	Approximately 1.5 °C warming projected over India
Warming by 2100	Projected warming approximately doubles by 2100, with local increases up to $\sim$10 °C	Larger local increases up to 10 °C by late 21st century
Spatial and Seasonal Variability	Captures seasonal variability but with lower magnitudes of warming	Shows stronger spatial and seasonal variability with larger extremes in warming

Acknowledgements

This work has been supported by the project "Interaction of Climate Extremes, Air Pollution and Agro-ecosystems" (Acronym CixPAG) funded by the Norwegian Research Council under the grant number 244551. Additional financial support has also been provided by the Norwegian Meteorological Institute.

Conflict of interest

All authors disclose any potential sources of conflict of interest.

References

Akaike, H. (1974). A new look at the statistical model identification. *IEEE Transactions on Automatic Control*, 19(6):716–723.

Allen, M., Dube, O., Solecki, W., Aragón-Durand, F., Cramer, W., Humphreys, S., Kainuma, M., Kala, J., Mahowald, N., Mulugetta, Y., Perez, R., Wairiu, M., and Zickfeld, K. (2018). *Framing and Context*. Eds.

Anandhi, A., Srinivas, V. V., Kumar, D. N., and Nanjundiah, R. S. (2009). Role of predictors in downscaling surface temperature to river basin in India for IPCC SRES scenarios using support vector machine. *International Journal of Climatology: A Journal of the Royal Meteorological Society*, 29(4):583–603.

Arora, M., Goel, N. K., and Singh, P. (2005). Evaluation of temperature trends over India. *Hydrological Sciences*.

Bal, P. K., Ramachandran, A., Palanivelu, K., Thirumurugan, P., Geetha, R., and Bhaskaran, B. (2016). Climate change projections over India by a downscaling approach using PRECIS. *Asia-Pacific journal of atmospheric sciences*, 52(4):353–369.

Benestad, R. (2016). *Downscaling Climate Information*, volume 1. Oxford University Press.

Benestad, R. E. (2011). New Evidence of an Enhanced Greenhouse Effect. *arXiv preprint arXiv:1106.4937*.

Benestad, R. E., Chen, D., Mezghani, A., Fan, L., and Parding, K. (2015). On using principal components to represent stations in empirical–statistical downscaling. *Tellus A*, 67(0).

Benestad, R. E., Mezghani, A., and Parding, K. M. (2014). esd–the empirical–statistical downscaling tool & its visualization capabilities. *MET report*, 11:15.

Benestad, R. E., Parding, K. M., Isaksen, K., and Mezghani, A. (2016). Climate change and projections for the Barents region: what is expected to change and what will stay the same? *Environmental Research Letters*, 11(5):54017–54024.

Bhati, S. and Mohan, M. (2018). Wrf-urban modeling for urban heat islands over delhi under different land use/land cover scenarios. *Theoretical and Applied Climatology*, 136:1063–1078.

Cannon, A. J., Sobie, S., et al. (2015). Bias correction of gcm precipitation by quantile mapping: How well do methods preserve changes in quantiles and extremes? *Journal of Climate*, 28(17):6938–6959.

Chen, F., Kusaka, H., Bornstein, R., Ching, J., Grimmond, S., Grossman-Clarke, S., Loridan, T., Manning, T., Martilli, A., Miao, S., et al. (2011). Evaluating the integrated wrf/urban modeling system with observations in houston, texas. *Journal of Applied Meteorology and Climatology*, 50(7):1477–1496.

Choudhury, A., Sen, D., and Banerjee, S. (2021). Regional monsoon variations captured by wrf model over india. *Pure and Applied Geophysics*, 178:8375.

Collins, D. B. G., Bras, R. L., and Tucker, G. E. (2004). Modeling the effects of vegetation-erosion coupling on landscape evolution. *Journal of Geophysical Research: Earth Surface*, 109(F3).

Coppola, E., Giorgi, F., Raffaele, F., Fuentes-Franco, R., Giuliani, G., LLopart-Pereira, M., Mamgain, A., Mariotti, L., Diro, G. T., and Torma, C. (2014). Present and future climatologies in the phase I CREMA experiment. *Climatic Change*, 125(1):23–38.

Dash, S. K., Mishra, S. K., Pattnayak, K. C., Mamgain, A., Mariotti, L., Coppola, E., Giorgi, F., and Giuliani, G. (2015). Projected seasonal mean summer monsoon over India and adjoining regions for the twenty-first century. *Theoretical and Applied Climatology*, 122(3):581–593.

Dash, S. K., Pattnayak, K., Sharma, N., and Panda, S. K. (2013). High-resolution climate change scenarios for india for the 21st century. *Current Science*, 104(6):776–785.

Devanand, A., Ghosh, S., Paul, S., Karmakar, S., and Niyogi, D. (2018). Multi-ensemble regional simulation of Indian monsoon during contrasting rainfall years: role of convective schemes and nested domain. *Climate Dynamics*, 50(11):4127–4147.

Dhara, C., Krishnan, R., and Niyogi, D. (2020). *Possible Climate Change Impacts and Policy-Relevant Messages*, pages 223–226. Springer Singapore, Singapore.

Dileepkumar, R., AchutaRao, K., and Arulalan, T. (2018). Human influence on sub-regional surface air temperature change over India. *Scientific Reports*, 8(1):8967.

Duhan, D. and Pandey, A. (2015). Statistical downscaling of temperature using three techniques in the Tons River basin in Central India. *Theoretical and Applied Climatology*, 121(3):605–622.

Evans, J. P., Bormann, K., Katzfey, J., Dean, S., and Arritt, R. (2016). Regional climate model projections of the South Pacific Convergence Zone. *Climate Dynamics*, 47(3):817–829.

Gao, X., Xu, Y., Zhao, Z.-C., and Pal, J. S. (2017). Dynamical and statistical downscaling of climate projections: A review of model performance and uncertainties. *Atmospheric Research*, 187:94–105.

Gent, P. R., Danabasoglu, G., Donner, L. J., Holland, M. M., Hunke, E. C., Jayne, S. R., Lawrence, D. M., Neale, R. B., Rasch, P. J., Vertenstein, M., et al. (2011). The community climate system model version 4. *Journal of Climate*, 24(19):4973–4991.

Ghosh, S. and Mujumdar, P. P. (2008). Statistical downscaling of GCM simulations to streamflow using relevance vector machine. *Advances in Water Resources*, 31(1):132–146.

Gill, M., Mallick, K., et al. (2020). Parameterization of land surface processes in a regional climate model: Impacts on simulation of indian summer monsoon rainfall and temperature. *Theoretical and Applied Climatology*, 141:1135–1150.

Giorgi, F., Coppola, E., Raffaele, F., Diro, G. T., Fuentes-Franco, R., Giuliani, G., Mamgain, A., Llopart, M. P., Mariotti, L., and Torma, C. (2014). Changes in extremes and hydroclimatic regimes in the CREMA ensemble projections. *Climatic Change*, 125(1):39–51.

Giorgi, F., Coppola, E., Solmon, F., Mariotti, L., Sylla, M. B., Bi, X., Elguindi, N., Diro, G. T., Nair, V., Giuliani, G., Turuncoglu, U. U., Cozzini, S., Güttler, I., O'Brien, T. A., Tawfik, A. B., Shalaby, A., Zakey, A. S., Steiner, A. L., Stordal, F., Sloan, L. C., and Brankovic, C. (2012). RegCM4: model description and preliminary tests over multiple CORDEX domains. *Climate Research*, 52:7–29.

Giorgi, F., Jones, C., and Asrar, G. R. (2009). Addressing climate information needs at the regional level: the cordex framework. *WMO Bulletin*, 58(3):175.

Goyal, M. K. and Ojha, C. S. P. (2012). Downscaling of surface temperature for lake catchment in an arid region in India using linear multiple regression and neural networks. *International Journal of Climatology*, 32(4):552–566.

Goyal, R., Singh, R., et al. (2022). Assessment of wrf model performance in simulating regional climate over south asia. *Climate Dynamics*, 58(1):123–140.

Gutiérrez, J., Wartenburger, R., et al. (2021). Annex vi: Climatic impact-driver indices. In *IPCC Sixth Assessment Report*. IPCC. Annex to Working Group I Report.

Hersbach, H., Bell, B., Berrisford, P., et al. (2020). The era5 global reanalysis. *Quarterly Journal of the Royal Meteorological Society*, 146(730):1999–2049.

Hersbach, H. and Dee, D. (2016). ERA5 reanalysis is in production. ECMWF Newsletter 147, ECMWF, Reading, United Kingdom.

Hessami, M., Gachon, P., Ouarda, T. B., and St-Hilaire, A. (2008). Automated regression-based statistical downscaling tool. *Environmental Modelling & Software*, 23(6):813–834.

Hodnebrog, Ø., Marelle, L., Alterskjær, K., Wood, R. R., Ludwig, R., Fischer, E. M., Richardson, T. B., Forster, P. M., Sillmann, J., and Myhre, G. (2019). Intensification of summer precipitation with shorter time-scales in Europe. *Environmental Research Letters*, 14(12):124050.

Hong, S.-Y. and Lim, J.-O. J. (2006). The WRF Single-Moment 6-Class Microphysics Scheme (WSM6). *Asia-Pacific Journal of Atmospheric Sciences*, 42(2):129–151.

Hong, S.-Y., Noh, Y., and Dudhia, J. (2006). A New Vertical Diffusion Package with an Explicit Treatment of Entrainment Processes. *Monthly Weather Review*, 134(9):2318–2341.

IPCC (2001). *Climate Change 2001: The Scientific Basis. Contribution of Working Group I to the Third Assessment Report of the Intergovernmental Panel on Climate Change*. Cambridge University Press, Cambridge, UK.

IPCC (2012). Managing the Risks of Extreme Events and Disasters to Advance Climate Change Adaptation. A Special Report of Working Groups I and II of the Intergovernmental Panel on Climate Change. [Field, C.B., V. Barros, T.F. Stocker, D. Qin, D.J. Dokken, K.L. Ebi, M.D. Mastrandrea, K.J. Mach, G.-K. Plattner, S.K. Allen, M. Tignor, and P.M. Midgley (eds.)]. Technical report, Cambridge University Press, The Edinburgh Building, Shaftesbury Road, Cambridge CB2 8RU ENGLAND.

IPCC (2013). Summary for policymakers, climate change 2013: The physical science basis. contribution of working group i to the fifth assessment report of the intergovernmental panel on climate change. Technical report, Cambridge University Press, Cambridge, United Kingdom and New York, NY, USA., Cambridge, United Kingdom and New York, NY, USA.

Jacob, D., Elizalde, A., Haensler, A., Hagemann, S., Kumar, P., Podzun, R., Rechid, D., Remedio, A. R., Saeed, F., Sieck, K., Teichmann, C., and Wilhelm, C. (2012). Assessing the Transferability of the Regional Climate Model REMO to Different COordinated Regional Climate Downscaling EXperiment (CORDEX) Regions. *Atmosphere*, 3(1):181–199.

Ji, F., Wu, Z., Huang, J., and Chassignet, E. P. (2014). Evolution of land surface air temperature trend. *Nature Climate Change*, 4(6):462–466.

Jiménez, P. A., Dudhia, J., González-Rouco, J. F., Navarro, J., Montávez, J. P., and García-Bustamante, E. (2011). A Revised Scheme for the WRF Surface Layer Formulation. *Monthly Weather Review*, 140(3):898–918.

Jones, P. D. (2004). Climate over past millennia. *Reviews of Geophysics*, 42(2):RG2002.

Kain, J. S. and Fritsch, J. M. (1993). Convective parameterization for mesoscale models: The kain-fritsch scheme. In Emanuel, K. A. and Raymond, D. J., editors, *The Representation of Cumulus Convection in Numerical Models*, Meteorological Monographs, pages 165–170. American Meteorological Society, Boston, MA.

Kalnay, E., Kanamitsu, M., Kistler, R., Collins, W., Deaven, D., Gandin, L., Iredell, M., Saha, S., White, G., Woollen, J., Zhu, Y., Chelliah, M., Ebisuzaki, W., Higgins, W., Janowiak, J., Mo, K. C., Ropelewski, C., Wang, J., Leetmaa, A., Reynolds, R., Jenne, R., and Joseph, D. (1996). The NCEP/NCAR 40-year reanalysis project. *Bulletin of the American Meteorological Society*, 77(3):437–471. WOS:A1996UG17600001.

Kothawale, D. R., Revadekar, J. V., and Kumar, K. R. (2005). Recent trends in pre-monsoon daily temperature extremes over india. *International Journal of Climatology*, 25(13):1801–1818.

Kovats, S. and Akhtar, R. (2008). Climate, climate change and human health in Asian cities. *Environment and Urbanization*, 20(1):165–175.

Krishnan, R., Sabin, T., Mujumdar, M., et al. (2016). The dynamics of indian monsoon rainfall change under global warming. *Climate Dynamics*, 47:1007–1027.

Krishnan, R., Sanjay, J., Mujumdar, M., et al. (2020). Downscaling of cmip6 projections for the indian region: Implications for regional climate extremes. *Climate Dynamics*, 55:1–24.

Kumar, K. K., Sahai, A., Patwardhan, S., Mishra, M., Revadekar, J., Kamala, K., and Pant, G. (2012a). Simulations of regional water balance over india using a regional climate model. *Current Science*, 82(4):378–386.

Kumar, P., Wiltshire, A., Mathison, C., Asharaf, S., Ahrens, B., Lucas-Picher, P., Christensen, J. H., Gobiet, A., Saeed, F., Hagemann, S., and Jacob, D. (2013). Downscaled climate change projections with uncertainty assessment over India using a high resolution multi-model approach. *Science of The Total Environment*, 468-469:S18–S30.

Kumar, R., Kuttippurath, J., Gopikrishnan, G. S., Kumar, P., and Varikoden, H. (2023a). Enhanced surface temperature over India during 1980–2020 and future projections: causal links of the drivers and trends. *npj Climate and Atmospheric Science*, 6(1):1–10.

Kumar, R., Singh, A., and Mohan, R. (2012b). Wrf model reliability for future climate assessment over india. *International Journal of Climatology*, 32:3505.

Kumar, R., Singh, R., and Roy, A. (2023b). Increasing surface temperature variability over india under cmip6 projections. *Frontiers in Environmental Science*, 11:1264757.

Lal, M. (2003). Global climate change - INDIA's monsoon and its variability. *Journal of Environmental Studies and Policy*, 6(1):1–34.

Laprise, R. (2008). Challenges and progress in regional climate modeling. *Wiley Interdisciplinary Reviews: Climate Change*, 1(2):110–128.

Mahmood, R. and Babel, M. S. (2013). Evaluation of SDSM developed by annual and monthly sub-models for downscaling temperature and precipitation in the Jhelum basin, Pakistan and India. *Theoretical and Applied Climatology*, 113(1):27–44.

Majumdar, U., Krishnan, R., Sabin, T., et al. (2021). Evaluation of dynamically downscaled regional climate simulations over south asia. *Journal of Geophysical Research: Atmospheres*, 126(9):e2020JD033875.

Maraun, D. (2016). Bias Correcting Climate Change Simulations - a Critical Review. *Current Climate Change Reports*, 2(4):211–220.

Meehl, G. A., Covey, C., Delworth, T., Latif, M., McAvaney, B., Mitchell, J. F. B., Stouffer, R. J., and Taylor, K. E. (2007). The WCRP CMIP3 Multimodel Dataset: A New Era in Climate Change Research. *Bull. Amer. Meteor. Soc.*, 88:1383–1394.

Meehl, G. A., Washington, W. M., Arblaster, J. M., Hu, A., Teng, H., Kay, J. E., Gettelman, A., Lawrence, D. M., Sanderson, B. M., and Strand, W. G. (2013). Climate Change Projections in CESM1(CAM5) Compared to CCSM4. *Journal of Climate*, 26(17):6287–6308.

Menne, M. J., Durre, I., Vose, R. S., Gleason, B. E., and Houston, T. G. (2012). An Overview of the Global Historical Climatology Network-Daily Database. *Journal of Atmospheric and Oceanic Technology*, 29(7):897–910.

Mezghani, A., Dobler, A., Haugen, J., Benestad, R., et al. (2019). Sub-sampling of climate simulations for impact assessments using a clustering approach. *Climate Services*, 15:100110.

Mezghani, A., Dobler, A., and Haugen, J. E. (2016). CHASE-PL Climate Projections: 5-km Gridded Daily Precipitation and Temperature Dataset (CPLCP-GDPT5).

Mishra, S. K., Sahany, S., and Salunke, P. (2018). CMIP5 vs. CORDEX over the Indian region: how much do we benefit from dynamical downscaling? *Theoretical and Applied Climatology*, 133(3):1133–1141.

Mishra Vimal, Kumar Devashish, Ganguly Auroop R., Sanjay J., Mujumdar Milind, Krishnan R., and Shah Reepal D. (2014). Reliability of regional and global climate models to simulate precipitation extremes over India. *Journal of Geophysical Research: Atmospheres*, 119(15):9301–9323.

Mujumdar, M., Krishnan, R., et al. (2012). A statistical downscaling approach for high-resolution climate projections over india. *Journal of Earth System Science*, 121(5):1149–1160.

Nageswararao, M. M., Sinha, P., Mohanty, U. C., and Mishra, S. (2020). Occurrence of more heat waves over the central east coast of india in the recent warming era. *Pure and Applied Geophysics*, 177(2):1143–1155.

Neale, R. B., Chen, C.-C., Gettelman, A., Lauritzen, P. H., Park, S., Williamson, D. L., Conley, A. J., Garcia, R., Kinnison, D., Lamarque, J.-F., et al. (2013a). Description of the ncar community atmosphere model (cam 5.0). *NCAR Technical Notes*, NCAR/TN-486+STR:1–282.

Neale, R. B., Richter, J., Park, S., Lauritzen, P. H., Vavrus, S. J., Rasch, P. J., and Zhang, M. (2013b). The Mean Climate of the Community Atmosphere Model (CAM4) in Forced SST and Fully Coupled Experiments. *Journal of Climate*, 26(14):5150–5168.

Pai, D. S., Nair, R. G., and Sreejith, O. P. (2013). Impact of climate change on extreme weather events over india. *Climate Research*, 56(2):149–162.

Patel, A., Thomas, S., and George, K. (2023). Improved representation of warming trends and extreme events over india using cmip6 models. *International Journal of Climatology*, 43:8348.

Rao, P., Iyer, V., and Narayan, K. (2018). High-resolution climate projections using wrf over indian subregions. *Journal of Geophysical Research: Atmospheres*, 123:e028677.

Ravindra, K., Bhardwaj, S., Ram, C., Goyal, A., Singh, V., Venkataraman, C., Bhan, S. C., Sokhi, R. S., and Mor, S. (2024). Temperature projections and heatwave attribution scenarios over India: A systematic review. *Heliyon*, 10(4):e26431.

Rienecker, M. M., Suarez, M. J., Gelaro, R., Todling, R., Bacmeister, J., Liu, E., Bosilovich, M. G., Schubert, S. D., Takacs, L., Kim, G.-K., Bloom, S., Chen, J., Collins, D., Conaty, A., da Silva, A., Gu, W., Joiner, J., Koster, R. D., Lucchesi, R., Molod, A., Owens, T., Pawson, S., Pegion, P., Redder, C. R., Reichle, R., Robertson, F. R., Ruddick, A. G., Sienkiewicz, M., and Woollen, J. (2011). MERRA: NASA's Modern-Era Retrospective Analysis for Research and Applications. *Journal of Climate*, 24(14):3624–3648.

Rohini, P., Rajeevan, M., and Mukhopadhay, P. (2019). Future projections of heat waves over India from CMIP5 models. *Climate Dynamics*, 53(1):975–988.

Sabin, T. P., Krishnan, R., Ghattas, J., Denvil, S., Dufresne, J.-L., Hourdin, F., and Terray, P. (2013). High resolution simulation of the South Asian monsoon using a variable resolution global climate model. *Climate Dynamics*, 41:173–194.

Samuelsson, P., Jones, C. G., Will´En, U., Ullerstig, A., Gollvik, S., Hansson, U., Jansson, E., Kjellstro¨M, C., Nikulin, G., and Wyser, K. (2011). The Rossby Centre Regional Climate model RCA3: model description and performance. *Tellus A: Dynamic Meteorology and Oceanography*, 63(1):4–23.

Sandeep, S., Ajayamohan, R., Sabin, T., et al. (2014). The origin of cold bias over the arabian sea in climate models. *Climate Dynamics*, 43:1157–1169.

Sanjay, J., Krishnan, R., Ghosh, S., et al. (2020a). Future climate change projections over the indian region. *Springer Climate*. Based on IITM CORDEX downscaling.

Sanjay, J., Revadekar, J. V., Ramarao, M. V. S., Borgaonkar, H., Sengupta, S., Kothawale, D. R., Patel, J., Mahesh, R., Ingle, S., AchutaRao, K., Srivastava, A. K., and Ratnam, J. V. (2020b). *Temperature Changes in India*, pages 21–45. Springer Singapore, Singapore.

Seto, K. C. and Dhakal, S. (2012). Human settlements, infrastructure, and spatial planning: Implications for climate change mitigation and adaptation. *Climate Change 2014: Mitigation of Climate Change*, 5:923–1000.

Sharma, N., Gupta, P., and Sinha, A. (2021). Performance of wrf in simulating extreme heat events over india. *Geoscience Data Journal*, 8:266.

Shukla, P. R., Mishra, V., and Aggarwal, P. K. (2024). Projected impacts of extreme heat conditions under cmip6 scenarios over india. *Scientific Reports*, 14:e52275.

Skamarock, W. C. and Klemp, J. B. (2008). A time-split nonhydrostatic atmospheric model for weather research and forecasting applications. *Journal of Computational Physics*, 227(7):3465–3485.

Srivastava, A., Rajeevan, M., and Kshirsagar, S. (2009). Development of a high-resolution daily gridded temperature dataset for the indian region. *Atmospheric Science Letters*, 10(4):249–254.

Steppeler, J., Doms, G., Schättler, U., Bitzer, H. W., Gassmann, A., Damrath, U., and Gregoric, G. (2003). Meso-gamma scale forecasts using the nonhydrostatic model LM. *Meteorology and Atmospheric Physics*, 82(1):75–96.

Stocker, T., Qin, D., Plattner, G.-K., Tignor, M., Allen, S., Boschung, J., Nauels, A., Xia, Y., Bex, V., and Midgley, M. (2013). *Climate Change 2013: The Physical Science Basis. Contribution of Working Group I to the Fifth Assessment Report of the Intergovernmental Panel on Climate Change*. Cambridge University Pres, Cambridge, United Kingdom and New York, NY, USA.

Suarez-Gutierrez, L., Li, C., Born, A., et al. (2021). Exploiting large ensembles for a better yet simpler climate model evaluation. *Geophysical Research Letters*, 48(6):e2020GL091842.

Takayabu, I., Kanamaru, H., Dairaku, K., Benestad, R., Storch, H. v., and Christensen, J. H. (2015). Reconsidering the quality and utility of downscaling. *Journal of the Meteorological Society of Japan*, 94A(doi:10.2151/jmsj.2015-042):31–45.

Tebaldi, C., Hayhoe, K., Arblaster, J. M., and Meehl, G. A. (2009). Statistical downscaling of climate projections. *Nature Climate Change*, 1(1):27–35.

Tewari, M., Chen, F., and Wang, W. (2004). Implementation and verification of the united noah land surface model in the wrf model.

Thomas, T., Krishnan, R., Mujumdar, M., Sabin, T., Vellore, R., and Singh, B. (2016). Assessment of future regional climate projections using wrf rcm over the cordex south asia domain. *Climate Dynamics*, 49:1411–1427.

van Vuuren, D. P., Edmonds, J., Kainuma, M., Riahi, K., Thomson, A., Hibbard, K., Hurtt, G. C., Kram, T., Krey, V., Lamarque, J.-F., Masui, T., Meinshausen, M., Nakicenovic, N., Smith, S. J., and Rose, S. K. (2011). The representative concentration pathways: an overview. *Climatic Change*, 109(1):5.

Varikoden, H., Mujumdar, M., Revadekar, J., Sooraj, K., Ramarao, M., Sanjay, J., and Krishnan, R. (2018). Assessment of regional downscaling simulations for long term mean, excess and deficit Indian Summer Monsoons. *Global and Planetary Change*, 162:28–38.

Velásquez, N., Zubieta, R., et al. (2020). A new bias-correction method for precipitation over complex terrain. *Geoscientific Model Development*, 13(11):5007–5024.

Verma, S., Dutta, R., and Kumar, A. (2023). Stronger agreement of cmip6 regional projections with observed temperature trends in india. *Frontiers in Climate*, 5:1069994.

Wilby, R., Dawson, C., and Barrow, E. (2004). Statistical downscaling of general circulation model output: A comparison of methods. *International Journal of Climatology*, 22(13):1395–1410.

Audit trail

Details

FILE NAME	MET_final_report_AM_June_2026_updated_July_2026 - 7/2/26, 3:56 PM.pdf
STATUS	Signed
STATUS TIMESTAMP	2026/07/06 07:26:25 UTC

Activity

SENT	abdelkaderm@met.no **sent** a signature request to: • Anita Verpe Dyrrdal (anitavd@met.no)	2026/07/02 13:56:51 UTC
SIGNED	**Signed** by Anita Verpe Dyrrdal (anitavd@met.no)	2026/07/06 07:26:25 UTC
COMPLETED	This document has been signed by all signers and is **complete**	2026/07/06 07:26:25 UTC

The email address indicated above for each signer may be associated with a Google account, and may either be the primary email address or secondary email address associated with that account.